A New V_s-Based Liquefaction Triggering Procedure for Gravelly Soils

2 Kyle M. Rollins

- 3 Prof., Civil and Environ. Engr. Dept., Brigham Young Univ., 430 Engineering Bldg., Provo, UT
- 4 84602, ORCID: https://orcid.org/0000-0002-8977-6619, email: rollinsk@byu.edu

5

1

- 6 Jashod Roy
- 7 Ph.D. Candidate, Civil & Environ. Engr. Dept., Brigham Young Univ, 430 Engineering Bldg.,
- 8 Provo, UT 84602, ORCID: https://orcid.org/0000-0003-0854-3790, email:
- 9 jashod.roy@gmail.com

10 11

- Adda Athanasopoulos-Zekkos
- 12 Assist. Prof., Civil Engr. Dept., Univ. of California, Berkeley, Berkeley, CA,ORCID: https://or-
- cid.org/0000-0002-3785-9009, email: adda.zekkos@berkeley.edu

14

- 15 Dimitrios Zekkos
- Assoc. Prof., Civil. Engr. Dept. univ. of California, Berkeley, CA, ORCID: https://or-nto.nc/
- 17 <u>cid.org/0000-0001-9907-3362</u>, email: <u>zekkos@berkeley.edu</u>

18 19

- Sara Amoroso
- Assist. Prof., Dept. of Engr. and Geology, University of Chieti-Pescara, Viale Pindaro, 42, 65129
- 21 Pescara, ITALY, ORCID: https://orcid.org/0000-0002-8977-6619, email:
- 22 <u>sara.amoroso@unich.it</u>; Roma 1 Section, Istituto Nazionale di Geofisica e Vulcanologia, Viale
- 23 Crispi, 42, 67100, L'Aquila, ITALY

2425

- Zhenzhong Cao
- 26 Prof., Guangxi Key Laboratory of Geomechanics and Geotech. Engrg., Guilin University of
- 27 Technology, Guilin 541004, CHINA, https://orcid.org/0000-0001-9138-3390, email: iem-
- 28 <u>czz@163.com</u>

29

- 30 Giuliano Milana
- 31 Technologist, Roma 1 Section, Istituto Nazionale di Geofisica e Vulcanologia, Via di Vigna
- 32 Murata, 605, 00143, Rome, Italy. ORCID: https://orcid.org/0000-0002-2775-4924, email:
- 33 giuliano.milana@ingv.it,

3435

- Maurizio Vassallo
- 36 Researcher, Roma 1 Section, Istituto Nazionale di Geofisica e Vulcanologia, Viale Crispi, 43,
- 37 67100 L'Aquila, Italy. ORCID: https://orcid.org/0000-0001-8552-6965, email:
- 38 maurizio.vassallo@ingv.it

39 40

- Giuseppe Di Giulio
- 41 Researcher, Roma 1 Section, Istituto Nazionale di Geofisica e Vulcanologia, Viale Crispi, 43,
- 42 67100 L'Aquila, Italy. ORCID: https://orcid.org/0000-0002-4097-7102, email: giuseppe.digiu-
- 43 lio@ingv.it

44 45

ABSTRACT

46

47

48

49

50

51

52

53

54

55

56

57

58

59

60

61

62

63

64

65

66

67

68

Liquefaction assessment has primarily been performed using in-situ penetration testing but this practice become problematic for gravelly soils. For example, SPT- or CPT-based correlations can become unreliable owing to interference with large-size gravel particles while the Becker Penetration Test, commonly used for gravelly soil, can be relatively expensive and requires conversion to an equivalent sand blow count. As an alternative, probabilistic liquefaction triggering curves have been developed based on shear wave velocity (V_s) using gravel sites in the M_w 7.9 Wenchuan earthquake. These curves have significant uncertainty because of the small data set. In this study, new probabilistic triggering curves for gravel liquefaction have been developed based on a V_s dataset. The dataset consists of 174 data points (96 liquefaction and 78 no liquefaction) obtained from 17 earthquakes in seven countries within different geological environments. The larger data set has better constrained the curves and reduced the range between the 15% and 85% probability of liquefaction curves, indicating less uncertainty. These triggering curves for gravel are shifted to the right relative to comparable curves for sand indicating that higher V_s values are necessary to preclude liquefaction. To account for the influence of the different earthquake magnitudes on liquefaction, a magnitude scaling factor (MSF) was developed specifically for gravel. This curve falls within the range of other MSF curves for sands based on V_s .

Author keywords: gravel liquefaction, probabilistic liquefaction triggering curve, shear wave velocity, magnitude scaling factor

INTRODUCTION

Liquefaction of loose saturated granular soils produces significant damage to civil infrastructure such as bridges, roadways, and ports in most major earthquakes. Liquefaction and the resulting loss of shear strength causes landslides, lateral spreading, bearing capacity failure for foundations, along with excessive settlement and rotation of foundations. Direct and indirect economic losses resulting from liquefaction are substantial costs to society. Evidence of gravel liquefaction has been reported in multiple case histories during 26 earthquake events over the past 130 years, as summarized in Table 1. Assessing the potential for liquefaction of gravelly soils in a cost effective and reliable way has often posed a significant challenge in geotechnical engineering.

Typical laboratory investigation techniques have proven to be ineffective for characterizing gravelly soil due to the cost and difficulty of extracting undisturbed sample from gravelly deposits (Cao et al. 2013). In addition, the large particle size of gravels can lead to artificially high penetration resistance values from traditional in situ test such as the cone penetrometer (CPT) test and the Standard Penetration (SPT) test (De Jong et al. 2017). The 168 mm diameter Becker Penetration Test (BPT) (Harder and Seed 1986, Harder 1997) reduces the potential for artificially high penetration values; however, this method is relatively expensive and is not available outside of North America. In addition, the method requires a correlation between the BPT blow count and the SPT blow count which leads to greater uncertainty relative to methods that are directly correlated with field liquefaction resistance.

As an alternative, in situ measurement of shear wave velocity (V_s) is a popular way of characterizing the liquefaction resistance of soil deposits. V_s is a basic mechanical property of soil materials, directly related to the small strain shear modulus (G_0), that is an essential parameter for performing soil-structure interaction analysis and liquefaction evaluation under earthquake loading. The use of V_s as an index of liquefaction resistance is based on the fact that V_s and liquefaction resistance are similarly influenced by void ratio, effective vertical stresses, stress history and geologic age (Youd et al. 2001). In addition, V_s is considerably less sensitive to the problems of soil compression and reduced penetration resistance when fines are present, compared with SPT and

CPT methods. Moreover, V_s only requires relatively minor corrections for fines content (FC) at least for sands (Kayen et al. 2013) unlike the SPT or CPT which needs significant correction for FC for liquefaction evaluation. The primary advantage of the in-situ V_s approach is that testing can be performed at sites where boring is not possible, or the penetration test results may be unreliable. Hence, V_s measurement can be considered as a reliable and economical alternative to overcome the difficulties of penetration testing through gravelly strata. Nevertheless, some concern exists about the applicability of V_s measurement for liquefaction assessment because V_s is essentially a small-strain parameter whereas liquefaction is a medium to large strain phenomenon (Jamiolkowski and Lo Presti 1990, Kramer et al. 1996). However, the ultimate strength, at large strain, typically increases as the initial shear stiffness increases and hence V_s may still be correlated with liquefaction resistance.

The traditional methods of measuring V_s require a penetrometer or instrumented boreholes to measure the travel time of shear waves at various depths. A downhole test requires one borehole to measure the vertically propagating wave, while a cross-hole test requires at least two boreholes to directly measure the horizontally propagating wave (Stokoe et al. 1994). These invasive test methods are usually quite expensive due to the cost of drilling, casing, and grouting boreholes. In the last two decades, some advanced non-invasive test methods (Spectral Analysis of Surface Waves (SASW) and Multichannel Analysis of Surface Wave (MASW) have been developed, which indirectly estimate the V_s profile using surface wave dispersion characteristics of the ground (Stokoe et al. 1994, Andrus 1994, Kayen et al. 2002). These non-invasive test methods can significantly reduce the cost of in-situ V_s estimation, although they are affected by uncertainties related to poor power in resolving very thin layers and very short wavelengths. They also

suffer from uncertainty in inverting the dispersion curve and become less reliable with depth below the ground surface (Vantassel and Cox, 2021). Despite these limitations, which also affect techniques based on body waves, the non-invasive techniques are a good compromise for deriving an average V_s profile at a rather low operational cost, especially at stiffer sites where penetration techniques are not possible. In fact, testing at three field test sites indicate that variability of V_s profiles from non-invasive methods were generally comparable to those from invasive methods when performed by experts (Garofalo et al. 2016b).

Dobry et al. (1982) proposed a strain-based approach for assessment of liquefaction potential and developed the concept of a cyclic threshold strain for which pore pressures are generated. To develop a more simplified method of liquefaction triggering analysis compatible with in-situ tests like the SPT or CPT, Seed et al. (1983) developed Cyclic Stress Ratio (CSR) - V_s triggering model using SPT vs. V_s correlations. Later, in the early 1990s, several correlations were developed between the effective stress normalized shear wave velocity (V_{s1}) and the Cyclic Resistance Ratio (CRR) causing liquefaction based on an increasing number of direct field measurements of V_s at liquefaction sites (Robertson et al. 1992, Kayen et al. 1992, Lodge 1994). These correlations were based on the liquefaction of sandy soils.

Andrus and Stokoe (2000) increased the population of V_s data by collecting a large database from locations around the world where both sandy and gravelly soils had liquefied in various seismic events. Based on this dataset, improved triggering curves were developed for sands and gravels for different FC percentages. The database of Andrus and Stokoe (2000) only contained a limited number of data points where the V_{s1} was higher than 200 m/s even for gravelly soils. This is consistent with observations by Kokusho et al. (1995) that loose gravels, even though well-graded,

can exhibit shear wave velocities similar to those of loose sands and can be susceptible to liquefaction. In contrast, the SPT- V_s correlation by Ohta and Goto (1978) and the correlation by Rollins et al. (1998b) suggest a higher range of V_{s1} (230 m/s) for liquefiable Holocene gravels. Such variation of shear wave velocity in gravelly soils can be due to variations in gravel content, grain size distribution and the relative density of the soil matrix (Kokusho et al. 1995, Weston 1996, Chang 2016, Chen et al. 2018). For example, a loose well graded gravel deposit and a medium dense to dense sand deposit can have a similar range of shear wave velocity.

Based on the Andrus and Stokoe (2000) dataset, Juang et al. (2001, 2002) developed probabilistic V_{s1} -based liquefaction triggering curves using reliability-based concepts. Kayen et al. (2013) subsequently developed V_s -based probabilistic liquefaction triggering curves for sandy soils by compiling a large database of 422 case histories of sand liquefaction. However, all these probabilistic correlations are based on the liquefaction of sands rather than gravels.

Using logistic regression techniques, Cao et al. (2011) produced liquefaction probability curves based on V_s data collected from the Chengdu plain in China where gravel liquefaction took place during the 2008 M_w 7.9 Wenchuan earthquake (Fig. 1a). These probability curves were based on 47 data points (19 liquefaction and 28 no liquefaction) based on a single earthquake and in a similar geological environment that consisted of loose alluvial fan gravel deposits that are typically overlain by a clay surface layer that is two to four meters thick (Cao et al. 2011). Owing to the limited number of data points and the possibility of false negatives (e.g. sites where liquefaction may have occurred but did not produce surface manifestation), the 15% and 85% probability of liquefaction triggering curves are relatively far apart. In comparison, V_s -based probabilistic liquefaction triggering curves for sands (Kayen et al. 2013) shown in Fig. 1b have more closely grouped 15 and 85% probability curves because of the much larger size of the dataset. Moreover, the Cao

et al. (2011) probability curves were developed for a single M_w 7.9 earthquake which made it impossible to develop appropriate correction factors for different earthquake magnitudes. Therefore, it was difficult to apply these triggering curves in evaluating the liquefaction potential of gravelly soils for earthquakes with different magnitudes. While existing MSF curves that were developed for sand liquefaction can be used (e.g. Youd et al. 2001), it is uncertain whether they would be appropriate for assessing gravel liquefaction based on V_s . Therefore, additional effort is necessary to collect more V_s data from the gravel liquefaction sites to improve the existing V_s -based liquefaction triggering curves for gravelly soils.

Hence in the present study, a larger database consisting of 174 data points have been compiled by collecting 127 additional data points from seven different countries around the world where gravel liquefaction did or did not take place in 17 major earthquake events and adding them to the existing 47 data points from China reported by Cao et al. (2011). Based on this new dataset, a new family of probabilistic liquefaction triggering curves was developed using logistic regression techniques. The triggering equations developed in the present study include the moment magnitude for each case history as an independent variable. This formulation made it possible to develop a new Magnitude Scaling Factor (MSF) curve expressly for gravel liquefaction based on V_s . This paper provides details regarding the collection and processing of the expanded dataset along with the development of the new liquefaction triggering procedure. The proposed V_s -based triggering curves are compared with existing V_s -based probabilistic triggering curves developed for gravel by Cao et al. (2011) as well those developed for sand by Kayen et al. (2013).

COLLECTION OF ADDITIONAL V_s-BASED CASE HISTORY DATA

As a part of this study, additional gravel liquefaction case history data has been obtained by performing or collecting in-situ V_s test data from sites around the world where gravelly soil

liquefaction has been identified. The sites, where gravel liquefaction features (e.g., surface ejecta of gravelly soils, lateral spreading, settlement manifestation etc.) were found, have been considered as liquefaction points. In addition, V_s data were also collected from sites where no liquefaction manifestation was observed in spite of having gravel layers below the water table. These no liquefaction points may provide an important constraint on the triggering curves. In some cases, these points were the same sites that might have liquefied during higher magnitude earthquake but did not produce any liquefaction effects for other smaller earthquake events. The sites for V_s testing were strategically selected to fill significant gaps in the data set. Among the no liquefaction cases, there may be some false negative points (Boulanger and Idriss 2014, Cao et al. 2013) which might have liquefied during the actual event but did not produce any surface manifestation due to the presence of a thick impermeable cap layer overlying the gravelly strata that could prevent the eruption of gravelly ejecta onto the surface. Besides, relatively small width of ground cracks and fissures may also hinder the eruption of relatively heavy and big gravel particles. These issues could not be properly captured only based on site investigations performed in the present study and remain as a source of uncertainty in developing the liquefaction triggering procedure.

182

183

184

185

186

187

188

189

190

191

192

193

194

195

196

197

198

199

200

201

202

203

Salient information for every site corresponding to each case history event are summarized in the supplemental Table S1 along with the relevant references. Further details for every site, including the soil profiles and damages caused by the liquefaction incidence, can be found in the respective references listed in the table. A summary of the gradation curves for the investigated sites is shown in Fig. 2 which provides an overall range of the particle size distribution for the potentially liquefiable gravelly deposits. Fig. 2 shows that the gravelly deposits contain 20% to 70% gtravel content according to the 4.75-mm gravel size criterion. The newly collect fed case

histories have been added to the existing Chinese data to form a large V_s -database of gravel liquefaction case histories. The expanded database consists of 174 case histories (96 liquefaction sites and 78 non-liquefaction sites) resulting from 17 different earthquakes in seven countries. This collection of data provides a 270% increase in the number of case histories relative to the database of Cao et al. (2011).

Although a large portion of the new data points come from China (Zhou et al. 2020), there are also 76 new case histories from seven other countries. The distribution of data collected from different countries is shown by the bar chart in Fig. 3. The gravelly deposits at ports and dams are primarily man-made fills, whereas other sites consist of natural deposits from alluvial fans, glacial outwash, and fluvial processes. A bar chart is provided in Fig. 4 to show the distribution of different types of soil deposits included in the gravel liquefaction case histories database. This figure indicates that the alluvial deposits and man-made fills have experienced larger number of gravel liquefaction incidents, whereas a relatively smaller number of incidents took place in the glacio-fluvial and fluvial deposits.

Performance of In-situ Tests to Collect Additional V_s Data

At many sites V_s testing was performed using the Multichannel Analysis of Surface Waves (MASW) method. The MASW method considers the dispersion of Rayleigh waves to generate an apparent phase-velocity dispersion relationship that is then used in an inversion analysis to derive a V_s profile. MASW surveys were performed using a linear array at each site composed of vertical geophones (4.5 Hz) spaced at 1 m intervals to increase resolution near the surface and 3 m intervals for greater depths. A sledge-hammer (usually 5.5. kg) striking on a plastic plate was used as the seismic source. The source was aligned to the geophones and located at several offsets (3 to 5) for each linear array. For each offset, a stack of three to five measurements was considered adequate

to increase the signal-to-noise ratio. The recorded phase offset of different frequency waves (f-k analysis) is used to develop a relationship between phase velocity and frequency (or wavelength) called a dispersion curve. Based on the dispersion curves, inversion analyses were conducted using the Park et al. (1999) methodology and typically without a priori subsurface information to derive a shear wave velocity model. It is well known that major differences in interpretation arise not from the dispersion analyses particularly, but from the inversion algorithm used to estimate the V_s profile from the dispersion curve. Therefore, the inversion process has a much stronger influence over the final V_s model compared to the dispersion curve generation method (Garofalo et al. 2016a). At some Italian sites (Avasinis and Bordano), two-dimensional arrays of 24 vertical geophones with a diameter of about 50 m were installed in addition to the MASW acquisition. For the array's configuration, 23 geophones were installed around two concentric circles (with radii of 12 m and 24 m, respectively) with a spacing between adjacent geophones of about 10 m. The last geophone was installed in the center of circles. These arrays acquired ambient seismic noise for at least 1.5 hours and the data were analyzed through the frequency-wavenumber (f-k) algorithm to define a more refined dispersion curve generally characterized by a higher resolution towards low frequencies (< 10 Hz), compared to that inferred from the linear MASW analysis. The surface-wave inversion is affected by non-uniqueness of the solution (Foti et al. 2009), and to better constrain the inversion procedure, a joint inversion of surface Rayleigh-wave dispersion curves and ellipticity curves derived from ambient vibration analyses (HVSR) was performed (Arai and Tokimatsu 2005; Picozzi et al. 2005) for some of the investigated sites. The HVSR curve (horizontal-to-vertical spectral ratios using ambient noise; Nogoshi and Igarashi, 1971; Nakamura 1989) was computed using ambient noise recorded for a few hours by collocated seismic stations,

227

228

229

230

231

232

233

234

235

236

237

238

239

240

241

242

243

244

245

246

247

248

249

using a three-components velocimeter with an eigen-frequency of 5 seconds. The HVSR curve was considered connected to the ellipticity of Rayleigh-wave during the inversion step, with the HVSR peak providing information on the fundamental resonance frequency of the site (Fäh et al. 2003).

This procedure, based on a joint inversion, helped extend the investigated frequency range toward lower frequency values and to reduce the ambiguities typical in velocity profile inversion (Tokimatsu 1997; Wathelet et al. 2004). A joint inversion, combining active and passive data analysis as well as any a-priori information, allows one, in principle, to increase the reliability of the estimates of the average shear-wave velocity profile, and to achieve a greater investigation depth compared to that obtained by inverting only the dispersion curve from active data (Bard et al. 2010). Details of these inversion analyses for every site to obtain the best estimate of V_s can be found in the corresponding reference given in the supplemental Table S1.

Besides MASW, other tests e.g., SASW, cross hole testing, down hole testing etc. have also been performed at several sites, as mentioned in Table S1, to obtain the V_s profile. The distribution of different test methods used to investigate the gravel case history data in the present study is plotted in Fig. 5. The plot shows that the highest percentage of the V_s data was obtained by performing MASW at sites in Alaska, China, Italy, Ecuador, Greece, and New Zealand. A major portion of the Chinese data (Zhou et al. 2020) was also obtained by performing SASW and down hole testing. Moreover, SASW testing was also performed at sites in Idaho by Andrus (1994). At a few sites in Alaska, Friuli and Idaho, cross hole testing was also performed. The seismic dilatometer was also used to measure V_s at one site in L'Aquila.

Data Interpretation and Selection of Critical Layers

The V_s values obtained by various in-situ methods were corrected for overburden pressure to obtain V_{s1} using the equation:

$$V_{s1} = V_s (P_a/\sigma'_{vo})^{0.25} \tag{1}$$

where σ'_{vo} is the initial vertical effective stress, and P_a is atmospheric pressure approximated by a value of 100 kPa as suggested by Sykora (1987) and adopted by Youd et al. (2001). These normalized V_{s1} profiles based on the V_s testing were then plotted as a function of depth. It should be noted that Liao and Whitman (1986) recommended Eq. 1 for sandy soils with a wide range of gradations and densities of soil matrix. Hence, the use of Eq. 1 to estimate the normalized shear wave velocity for gravelly soil is a reasonable approximation because the gravelly deposits contain a considerable sand content as shown by the gradation curves in Fig. 2. However, the correction factor may depend on a few other characteristics such as angularity, compressibility, crushing strength, etc. that might differ in the case of gravelly soil relative to sandy soil. To address these issues, exclusive investigation is required to explore the correction factors specifically for gravelly soils which is beyond the scope of the present study.

In addition, the *CSR* for each site and earthquake event was obtained by using the simplified equation:

$$CSR = 0.65 (a_{max}/g) (\sigma_{vo}/\sigma'_{vo}) r_d$$
(2)

Seed and Idriss (1971) developed Eq. 2 where σ_{vo} is the initial vertical total stress, a_{max} is the peak ground acceleration, and r_d is a depth reduction factor as reported in Youd et al (2001).

Peak ground accelerations (PGA or a_{max}) for each site were obtained either from nearby Strong Ground Motion Stations (SGMS) or from USGS Shake Maps (Worden et al. 2010) depending on the available data. This is a similar approach to that adopted by Idriss and Boulanger (2008) while developing CPT-based liquefaction triggering procedure for sandy soil. According to the references given in the supplemental Table S1, the *PGAs* at the sites of Manta, Hokkaido, Borah Peak, Wellington, Lixouri, and Argostoli were estimated from the nearby SGMS records. The PGA at the Chengdu Plain in China were obtained from the contour maps developed from the nearby SGMS records. At the Italian sites, the SGMS were located within the area of Avasinis but not close to the liquefied areas. Hence, the PGAs estimated from the nearby SGMS were verified with the results of a Ground Motion Prediction Equation, (GMPE) (Bindi et al. 2011) and USGS Shake Map estimations as reported in Rollins et al. (2020). At the sites in Alaska, PGAs were obtained from the USGS Shake Map. At the sites in L'Aquila, PGAs were determined using the SGMS for sites (Aquila3 and Aquila4) close to seismic station in operation during the earthquake, and using the information derived from the Shake Map (http://shakemap.rm.ingv.it/shake/index.html; Faenza and Michelini, 2011) for the remaining sites. Overall, 88% of PGA data are directly based on SGMS records and the remaining 12% are from USGS Shake Maps. It should be noted that estimation of PGA from different kinds of sources may add considerable uncertainty to the liquefaction potential evaluation. However, the fact that a large percentage of the PGAs in this study are based on direct measurement in the field can actually reduce the uncertainty to a moderate level.

290

291

292

293

294

295

296

297

298

299

300

301

302

303

304

305

306

307

308

309

310

311

312

Besides CSR, the moment magnitude (M_w) has been considered as another independent variable while developing the liquefaction triggering procedure. Values of M_w for all seismic events are also provided in the supplementary Table S1. The distribution of M_w versus PGA for all the data points is plotted in Fig. 6. It shows that the data set contains a broad range of M_w from 5.3

to 9.2 along with the PGAs varying from 0.116 to 1.457 g. In Fig. 6, there are several points which overlap each other that actually represent multiple sites for similar earthquake magnitude but different PGAs.

Based on the V_{s1} and CSR plots with the depth, the critical layer for each location has been identified as the layer which has the highest potential to trigger and manifest liquefaction at the ground surface (Cubrinovski et al., 2018). Typically, this was the gravelly layer corresponding to the lowest range of V_{s1} value below the water table (Kayen et al. 2013). There can be multiple critical layers along the depth which may be potentially liquefiable. Out of several possible layers, the representative critical layer for each borehole has been selected as that layer which is located at the closest to the water table being most likely to produce manifestation on the ground surface and has a minimum thickness of one meter to avoid the effect of thin peaks and troughs as suggested by Boulanger and Idriss (2014). Non-liquefiable cohesive soil layers were deliberately excluded from the critical layer consideration.

The distribution of V_{s1} with respect to the depth of critical layers for all the data points is illustrated by Fig.7. The plot shows that the critical gravel layers are mostly constrained within a depth of 14 m and the majority of the V_{s1} values for liquefiable strata remain less than about 300 m/s. This range of critical layer depth is consistent with some previous investigation results. For example, Youd et al. (2001) reported that the depth of the critical layers for most of the empirical SPT liquefaction data are less than 15 m. Likewise, Cubrinovski et al. (2017) noted that only one case history in the 250 CPT-based liquefaction case histories assembled by Boulanger and Idriss (2014) was located deep than 10 m. For the no liquefaction points, the V_{s1} values are distributed roughly from 180 m/s to 450 m/s. These no-liquefaction cases are a result of low CSR values, as

loose soil deposits may still not liquefy if the CSR is low. Therefore, the no-liquefaction points are distributed over a broader range of V_{s1} .

Limitations of the Collected Database

335

336

337

338

339

340

341

342

343

344

345

346

347

348

349

350

351

352

353

354

355

356

Besides shear wave velocity (V_s) , Cyclic Stress ratio (CSR) and moment magnitude (M_w) , there are other significant parameters e.g., percentage of fines, sand and gravel, relative density, hydraulic conductivity, thickness of impermeable cap layer overlying the gravelly strata etc. which may also play significant role in controlling the liquefaction resistance of gravelly soils. Fines content has already been included as an independent variable in developing V_s -based correlations for evaluating liquefaction potential of sands (Andrus and Stokoe 2000, Kayen et al. 2013). Unfortunately, the gravel liquefaction case histories collected in the present study do not have sufficient data for the critical layers to statistically formulate the influence of fines content (FC) on the liquefaction resistance. However, FC information has been included for some Japanese and Italian sites where specific information was available based on the sampling data. For many of the remaining sites, a range of FC data was available instead of specific sampling data for every V_s -testing location based on the range of gradation curves given in the respective reference (Fig. 3) and those FC ranges have also been included in the supplementary table. In addition to the fines content, the percentage of sand (SC) and gravel (GC) along with the relative density significantly control the shear wave velocity (V_s) of gravelly strata. Chang (2016) semi-empirically correlated V_s with GC and evaluated the liquefaction resistance of gravelly sand using the GC-corrected V_s . According to Chang (2016), the liquefaction resistance of gravelly sand with GC less than a threshold value (30-60%), where the gravel particles are floating in the sand matrix, can be evaluated based on the V_s of the sand matrix by applying the GC correction factor. However, if the GC is higher than the threshold

value, V_s should be estimated based on the overall soil mixture instead of only the sand matrix in performing the liquefaction evaluation.

Zhou et al. (2020) developed a correlation between V_{s1} and GC for a wider range based on the V_s of the gravelly deposits at the Chengdu Plain in China after the 2008 Wenchuan earthquake. This correlation shows a wide variation between the upper and lower bound of the V_{s1} which can be attributed to variations in relative density in the soil strata. In the present study, the database given in the supplementary Table S1 contains average information on GC for most of the sites instead of specific data for every location except for the Chinese data from Zhou et al. (2020) whereas, information on relative density is not available due to the difficulty in undisturbed sampling at most of the sites. Hence, the parameter GC could not be considered in the regression analysis due to insufficient information regarding grain size distribution for all critical layers. Furthermore, the present database contains a wide range of GCs where the GC-correction factor (Chang 2016) is not applicable for obtaining an equivalent liquefaction evaluation for sandy soil. However, the in-situ measured V_{s1} which has been included as the primary variable in the development of triggering curves can be considered as a combined function of all these parameters (GC, relative density) to account for their effect on the correlation.

Hydraulic conductivity is another parameter, independent of shear wave velocity (Zhou et al. 2020), which may significantly control the pore pressure generation in gravelly strata during seismic loading. As reported by Seed et al. (1976), gravelly soil with a hydraulic conductivity greater than about 0.3 cm/sec is unlikely to liquefy due to rapid dissipation of pore water pressure. However, the presence of an impermeable cap layer on top of the gravelly strata, as found in many of the case histories considered in the present study (e.g., Cao et al. 2012, Yegian et al. 1984, Rollins et al. 2020) may hinder the dissipation of pore pressure during an earthquake and cause

the triggering of liquefaction in the gravelly strata (Chen et al. 2018). In addition, an impermeable cap layer can also reduce the effect of liquefaction manifestation at the surface. In some cases, this may lead to a site being classified as a "no-liquefaction site" even though liquefaction may have occurred in the ground. This, of course, is a source of uncertainty for all available liquefaction triggering curves. On the other hand, without the presence of any overlying impervious cap, gravelly soil matrix classified as per the Unified Soil Classification System could still have sufficiently low hydraulic conductivity to generate high excess pore pressure and cause liquefaction during an earthquake event. For example, She et al. (2006) observed that gravel-sand mixtures having more than about 30% of sand typically have hydraulic conductivities that are similar to that of sandy soils. Furthermore, DeJong et al. (2017) reported that the permeability of sand- gravel mixtures is often low enough to generate excess pore pressures in earthquakes because the permeability is controlled by the D_{10} size, as noted by the Kozeny-Karmen equation (Kozeny 1927), which is controlled by the sand content.

A summary of the average grain size distribution curves for the present data set, shown in Fig. 2, indicates that most gravelly sites have a high sand content and small D_{10} size which are enough to keep the hydraulic conductivity below the threshold for triggering liquefaction during earthquake shaking. Therefore, the presence of an impermeable layer on top of the gravelly strata is not necessary to restrict the dissipation of pore water pressure and induce liquefaction. However, the available data regarding the hydraulic conductivity and other parameters controlling the generation of pore pressure are still insufficient to be included in statistical regression analyses for developing a new liquefaction triggering framework.

LIQUEFACTION EVALUATION BY EXISTING V_s -BASED TRIGGERING PROCE-DURE OF CAO ET AL. (2011)

The collected dataset given in the supplementary Table S1 provides an opportunity to evaluate the performance of the existing V_s -based triggering curves of Cao et al. (2011) for predicting the liquefaction potential of gravelly soils. The Cao et al. (2011) triggering curves were developed for a single earthquake event of M_w 7.9. Therefore, to perform the liquefaction assessment for the new database having a variety of earthquake magnitudes, the original triggering curves of Cao et al. (2011) have been modified to a M_w 7.5 earthquake reference standard using MSF factors given by the following equation which is reported in Youd et al. (2001).

$$MSF = 10^{2.24} / M_w^{2.56} \tag{3}$$

Hence, the modified form of the probability of liquefaction (P_L) is given by Eq. 4

412
$$P_L = \frac{1}{1 + exp(-11.97 + 0.039V_{s1} - 1.77LnCSR_{M=7.5})}$$
 (4)

413 where, $CSR_{M=7.5}$ is obtained by Eq. 5

$$CSR_{M=7.5} = CSR/MSF \tag{5}$$

Rearranging Eq. 4, the *CRR* at M_w 7.5 can be expressed as:

416
$$CRR_{M=7.5} = exp\left\{\frac{11.97 + 0.039V_{s,1} - ln\left(\frac{1 - P_L}{P_L}\right)}{1.17}\right\}$$
 (6)

Using Eq. 6, the modified set of triggering curves have been obtained for 15%, 30%, 50%, 70% and 85% probability of liquefaction. In addition, the CSRs of all the data points having different earthquake magnitudes have also been converted to M_w 7.5 using Eq 5. For each data point, the converted CSR has been plotted with the corresponding V_{s1} along with the modified triggering

curves, as shown in Fig. 8, to illustrate the comparison at the same magnitude standard. Liquefaction data points are shown with solid symbols while no-liquefaction data points are shown with open symbols.

Fig. 8 shows that most of the newly added liquefaction points with probabilities of liquefaction greater than 50% are satisfactorily evaluated by the Cao et al. (2011) triggering curves. In contrast, the no-liquefaction points from the Port of Wellington (Cook Strait and Lake Grassmere earthquakes) and Argostoli (1983 earthquake) fall higher than the 30% triggering line. In other words, these sites are evaluated as potentially liquefiable but this is inconsistent because these sites did not liquefy during the actual seismic event. Furthermore, the no-liquefaction points from L'Aquila in Italy at the middle portion of the plot fall between the 30% and 50% triggering curve indicating a relatively high chance of liquefaction, whereas the gravelly deposits at these sites did not liquefy during the actual earthquake events.

In addition, a large number of no-liquefaction data points from Chengdu plain in China newly added from Zhou et al. (2020) during the Wenchuan earthquake fall considerably above 30% triggering line interpreting those points as potentially liquefiable. Because the existing Cao et al. (2011) triggering curve incorrectly predicts liquefaction for a significant number of cases where no liquefaction occurred, a new set of triggering curves needs to be developed, based on the expanded data set, to provide a better assessment of liquefaction observed in the field case histories. Based on the additional data points, the spread in the triggering curves from 15% to 85% may also become narrower as false negatives and false positives (sites with cracking but without ejecta) become a smaller percentage of the total dataset.

DEVELOPMENT OF NEW PROBABILISTIC TRIGGERING CURVES

In this study, a logistic regression analysis (Liao et al. 1988, Youd and Noble 1997, Cao et al. 2011 and 2013, Rollins et al. 2021) has been performed to obtain a new set of probabilistic liquefaction triggering curves based on the whole database given in the supplementary Table S1. Unlike the correlation of Cao et al. (2011) which involved only one seismic event, the moment magnitude (M_w) has been considered to be an independent variable along with the other explanatory variables i.e. normalized shear wave velocity (V_{s1}) and the natural log of the cyclic stress ratio [Ln(CSR)] while performing the logistic regression analysis. To compute the CSR, the formulation of r_d in Eq. 2 has been updated to Eq. 7 to include the effect of magnitude on the variation of r_d with depth.

$$r_d = e^{\left[\alpha(z) + \beta(z)M_W\right]} \tag{7}$$

453 where

442

443

444

445

446

447

448

449

450

451

457

454
$$\alpha(z) = -1.012 - 1.126 \sin(\frac{z}{11.73} + 5.133)$$
 (8)

455
$$\beta(z) = 0.106 + 0.118sin(^{Z}/_{11.28} + 5.142)$$
 (9)

and z is the depth in meters, as proposed by Golezorkhi (1989) and Idriss (1999).

Regression Model

According to the logistic regression analysis procedure, the probability of occurring liquefaction (P_L) is expressed by the general equation,

460
$$P_L(\theta, X) = \frac{1}{1 + exp(\theta_1 X_1 + \theta_2 X_2 + \dots + \theta_n X_n)}$$
 (10)

where the series of X values represents the soil and the earthquake parameters. In this study, these variables are V_{s1} , M_w , and Ln(CSR) along with various combinations of these primary variables.

The vectors ' θ ' are the model coefficients, which are unknowns that need to be estimated to define the function of probability of liquefaction (P_L). These parameters have been obtained by using the maximum likelihood estimation (MLE) technique. The likelihood function can be expressed as:

466
$$L(\theta, X) = \prod [P_L(\theta, X)]^n [1 - P_L(\theta, X)]^{m-n}$$
 (11)

where *m* = total number of data in the sample, *n* = total number of liquefied sites i.e. *m*-*n* = total number of non-liquefied sites. To maximize this likelihood function, the following condition should be satisfied.

$$\frac{\partial L(\theta, X)}{\partial \theta_i} = 0; i = 1, 2, \dots, n \tag{12}$$

By satisfying Eq. 12, 'n' number of equations can be obtained which need to be solved to estimate the model coefficients '\theta'. However, solving this set of equations requires extensive numerical programming that has been accomplished by simply using the Variable Selection Procedure (Youd and Noble 1997) with the JMP Pro 13 software package in the present study. A similar approach was taken by Rollins et al. (2021) to develop the liquefaction triggering procedure based on the Dynamic Penetration Test (DPT) penetration resistance. However, a brief illustration of the logistic regression analysis associated with the stepwise variable selection procedure following the approach of Rollins et al. (2021) is given below.

Step 1: First a set of explanatory variables is defined by combining normalized shear wave velocity (V_{s1}) and earthquake parameters $(LnCSR \text{ and } M_w)$ in different forms. The explanatory variables in the first set are $[V_{s1}, V_{s1}^2, V_{s1}^3, V_{s1}^4, M_w, LnCSR]$ and different combinations of these variables such as $M_wLn(CSR)$, M_wV_{s1} , $V_{s1}Ln(CSR)$ etc. Hence, the likelihood function is formulated as a function

of this set of variables as given by Equation 11 and the first cycle of regression is performed to estimate the first set of model parameters based on Eq. 12.

Step 2: After the completion of the first cycle, Chi-square test results and P-values (the probability that the level of prediction of the model would decrease if the explanatory variable provided zero contribution to the model) are checked for the estimated model parameters for all the variables. The variable having the maximum P-value and minimum Chi-square value is eliminated from the set of explanatory variables as a high P-value essentially indicates that the associated variable adds the least contribution to the predictive capacity of the model. Hence, after eliminating the variable with the highest P-value, a new regression analysis is performed based on the new set of variables following step 1.

Step 3: Step 1 and 2 are repeated iteratively and the insignificant variables are excluded from the prediction model after each cycle of regression based on the Chi-square test and probability values. These cycles of regression are performed until the probability values of all the explanatory variables remaining in the model become less than 0.05.

Analysis Results and Discussion

Following steps 1 through 3, different forms of equations including lower to higher degrees of polynomials in V_{s1} , M_w and Ln(CSR) were obtained. The estimates of model parameters for these different forms are summarized in Table 2. The set of results shows that no combination of the basic explanatory variables was found to be statistically significant. Although, all the solutions given in Table 2 are statistically admissible, there are slight variations in their performance in evaluating the liquefaction and no liquefaction points of various range. To illustrate this fact, 30%

triggering line for all of the different solutions have been plotted together with all the points in Fig. 9.

Fig. 9 shows that the triggering curve based on the solution of trial 1 which is a function of only a first order polynomial in V_{s1} , starts with a much lower range of CRR that does not properly evaluate several no-liquefaction points at the low range of V_{s1} . The triggering curve obtained from the solution of trial 2 which contains a second order polynomial in V_{s1} is much improved compared to the first order solution at the lower range, but it becomes a little slanted towards right at the upper end of the curve which may show some limitations in evaluating the "no-liquefaction points" at the high range of V_{s1} . On the other hand, the trial 4 solution having V_{s1} polynomial up to the fourth order makes the triggering curve too steep and vertical from the middle to high range of CRR which may produce limitations in evaluating some "liquefaction" points in the middle or higher range of CSR. Hence by judging the performance of all these curves for the given data set, the trial 3 solution based on a third order polynomial of V_{s1} was determined to be the most suitable way of determining the liquefaction potential of the existing points in a reliable manner. Therefore, the recommended equation for obtaining the probability of liquefaction from this updated regression analysis is given by

$$520 P_L = \frac{1}{1 + exp\{1.6M_w + 4.95Ln(CSR) - 3.88x10^{-7}V_{s1}^{3}\}} (13)$$

Rearranging Eq. 13, the revised *CRR* can be written in the following form:

522
$$CRR = exp\left\{\frac{3.88x10^{-7}V_{s1}^{3} - 1.6M_{w} - ln\left(\frac{1-P_{L}}{P_{L}}\right)}{4.95}\right\}$$
 (14)

Substituting $M_w = 7.5$ and various probabilities of liquefaction, the relationship between V_{s1} and CRR can be obtained.

DEVELOPMENT OF MAGNITUDE SCALING FACTOR

While comparing the data points with the Cao et al. (2011) triggering curves, the original CSRs for all the points with various M_w values were converted to $CSR_{M=7.5}$ using Eq. 5, the lower bound MSF curve (Idriss, 1999) recommended by the NCEER/NSF workshop (Youd et al. 2001). However, the Idriss (199) MSF equation was primarily developed for the liquefaction of sand which could be a potential reason behind improper liquefaction assessment of several gravel liquefaction case histories using the Cao et al. (2011) triggering curves. However, in the new liquefaction triggering procedure described in the previous section, the moment magnitude, M_w , has been considered as a separate variable as shown in Eq. 13 and 14. Therefore, as a part of this regression analysis, a new MSF model has been developed specifically for gravelly soils that may help improve liquefaction assessment at some gravelly sites considered in the present study. However, more data from other earthquakes would still be desirable to refine the regression model and further constrain the set of triggering curves.

To develop the MSF curve, CSR values were first obtained from Eq. 14 for M_w 5.5 through 9 with an increment of 0.5 keeping V_{s1} and P_L constant. Then the CSRs for different magnitudes were divided by the $CSR_{M=7.5}$ to obtain the magnitude scaling factor. The same process was then repeated for different values of V_{s1} and P_L in Eq. 16 to obtain the variation of MSF with these variables. But notably, the MSF pattern did not vary with the normalized shear wave velocity (V_{s1}) and the probability of liquefaction (P_L). Hence, the MSF was found to be formulated as a function of magnitude with the best-fit exponential equation given by:

$$MSF = 10.667exp(-0.316M_w) (15)$$

The MSF curve obtained with Eq. 15 is plotted and compared with several other MSF curves in Fig. 10. The comparison shows that the MSF model developed for gravelly soil falls about mid-way between the Andrus and Stokoe (2000) curve at the high end and the Kayen et al. (2013) curve at the low end which were both developed for sandy soil based on V_{s1} . In addition, the MSF curve from this study falls just below the lower-bound range for MSF recommended by the NCEER/NSF liquefaction workshop (Youd et al. 2001, but a little higher than the MSF curve proposed by Idriss and Boulanger (2008). Hence, the MSF model developed in this study for gravelly soil appears to be reasonably consistent with existing MSF curves for sands.

Based on the new MSF model (Eq. 15), the CSRs for all the case history data points have been converted to $CSR_{M=7.5}$ and plotted with the newly developed triggering curves obtained by Eq. 14 as shown in Fig.11. Fig. 11 depicts that all the data points have been slightly relocated and the liquefaction potential of the marginal points are evaluated relatively better as compared to Fig.8. This fact is particularly applicable for the case histories at the port of Wellington in New Zealand and at the port of Argostoli in Cephalonia, Greece where liquefaction and no-liquefaction data points are now better distributed with respect to the 50% probability curve. Moreover, the larger database including the additional liquefaction and no-liquefaction data points have better constrained the triggering curves by reducing the uncertainty at both the higher and lower range of CSR. Therefore, the newly developed V_s -triggering procedure in association with the new MSF model provides a much improved alternative for evaluating the liquefaction potential of gravelly deposits.

COMPARISON WITH THE CAO ET AL. (2011) TRIGGERING CURVES

The newly developed probabilistic triggering curves with liquefaction probabilities of 15% to 85% are plotted in Fig. 12(a) with solid lines along with the similar curves developed by Cao et

al. (2011) marked as dashed lines to draw a distinct comparison between the two triggering procedures. For lower values of V_{s1} (around 150 m/s), the *CRR* for the new 50% probability of liquefaction curve is about 0.10 while it is only 0.04 for the Cao et al. (2011) curves. This adjustment produces much better agreement with observed field performance. This higher *CRR* values at lower shear wave velocities are also more typical of that predicted by the V_s -based triggering curves developed by Kayen et al. (2013) for sands. In fact, it can be seen from Fig. 11 that the marginal liquefaction and no-liquefaction points from the Port of Wellington for the 2013 Cook Strait and Lake Grassmere event of $M_w = 6.6$, the "no-liquefaction" points from Argostoli, KNK and Coyote Creek have played a significant role in constraining the lower branch of the triggering curves to move upwards. Likewise, the triggering curves at the higher range of V_{s1} have been tightened and slightly steepened compared to the Cao et al. (2011) triggering curves by the additional "no liquefaction" data points from Chengdu, L'Aquila and Valdez. However, more data points would certainly be desirable to better constrain the shape of the triggering curves in the high range of V_{s1} .

In the middle range of the triggering curves, there are a few "no liquefaction" points from the Chengdu plain that fall above the 50% triggering curve and a few liquefaction points from the same region the fall below the 30% triggering curve. Because of these points, the set of triggering curves remains slightly sloped above the V_{s1} value of 200 m/s causing several "no liquefaction" points to fall marginally on the 30% triggering curve instead of falling distinctly below this line. These points may belong to the false negative or false positive categories, as explained previously, leading to inconsistent evaluation of the actual incident. These points might also be governed by some other in-situ parameters such as the permeability of the soil strata, amount of fines content, presence of impervious cap layer etc. which have not been included in the regression analysis due

to the lack of information available for each site. These points remain as a source of uncertainty in the overall liquefaction triggering procedure.

As shown in Fig. 12a, for V_{s1} values above 200 m/s, the $P_L = 50\%$ curve for the new regression is very similar to that for the Cao et al. (2011) regression. However, the addition of new liquefaction points has pulled the new $P_L = 85\%$ curve to the right while the addition of no-liquefaction data points has pulled the new $P_L = 15\%$ curve to the left, relative to the Cao et al. (2011) curves. Moving the new $P_L = 15\%$ curve to the left is particularly significant because this curve is often recommended for deterministic evaluations (Kayen et al. 2013). However, the slope of the new set of curves from this study remain almost the same as for the Cao et al. (2011) curves. Overall, the spread between the triggering curves has been substantially reduced in comparison to the Cao et al. (2011) triggering curves. This outcome is consistent with the concept that the increased number of data points reduces the uncertainty that would develop for a limited number of individual data point that plots in an unexpected position. Furthermore, the addition of liquefaction and no-liquefaction data points have helped constrain the triggering curves.

COMPARISON WITH KAYEN ET AL. (2013) CURVES FOR SAND

A comparison is provided between the newly developed triggering curves for gravel and the curves developed by Kayen et al. (2013) for sand in Fig.12b. To plot the triggering curves for Kayen et al. (2013), an average effective vertical stress of 100 kPa, and fines content of 6% has been assumed to keep the values within a reasonable range. Although the probabilistic liquefaction triggering curves for gravel developed in this study are similar to those for sands (Kayen et al. 2013) at lower V_{s1} values typical of looser gravels, the curves diverge as V_{s1} increase. For example, V_{s1} equals 275 m/s for the proposed $P_L = 50\%$ curve for gravel in this study at a CRR of 0.5 in comparison with a V_{s1} of only 225 m/s for the $P_L = 50\%$ curve for sand proposed by Kayen et al.

(2013). This indicates that the probabilistic triggering curves for gravels from this study shift to the right relative to similar curves developed for sands as V_{s1} increases. This result indicates that gravels can still liquefy at V_{s1} values that would be high enough to preclude liquefaction in sand. This does not mean that gravels are more or less likely to liquefy than sand, it simply means that for a comparable level of shaking, a higher V_{s1} is necessary to obtain the same probability of liquefaction for sandy gravel than pure sand. This result is consistent with liquefaction case histories in gravels reported by Cao et al. (2011), Chang (2016), Rollins et al. (2020), and Zhou et al. (2020) where V_{s} -based triggering curves for sands would have incorrectly predicted no liquefaction, along with results from laboratory testing (e.g., Hubler et al. 2017 and 2018) as well.

SUMMARY AND CONCLUSION

In this study, probabilistic liquefaction triggering curves for gravelly soils based on the shear wave velocity (V_s) have been developed which can be used for liquefaction evaluation of gravelly soils for a wide range of earthquake magnitudes, tectonic settings, and geologic environments. These curves are a significant step forward compared to those developed by Cao et al. (2011), as the total number of data points has increased by 270%. V_{s1} data were compiled from various sites around the world where liquefaction or no liquefaction case histories of gravelly soils were observed during several earthquake events in the past. The expanded data set consists of 174 data points (96 liquefactions and 78 no liquefaction) during 17 different earthquakes in seven different countries in a variety of geological environments.

Based on the results of the field studies and data analysis performed in this study the following conclusions have ben drawn:

1. The increased number of liquefaction and no-liquefaction data points in the expanded dataset has better constrained the probabilistic liquefaction triggering curves. Relative to the

- Cao et al. (2011) curves, this has shifted the P_L = 85% curve to the right and P_L =15% curve to the left. The reduction in the range between the P_L = 85% and 15% curves indicates a considerable decrease in uncertainty, because false negative data points have less impact on the expanded data set. Shifting the P_L =15% curve to the left is significant because this probability curve is sometimes recommended for deterministic analyses (Kayen et al. 2013).
- 2. At lower V_{s1} value (≈ 150 m/s) typical of looser gravels, the proposed triggering curves for gravel in this study start at a higher range of CSRs compared to the curves developed by Cao et al. (2011). This modification was necessary to produce agreement with the no liquefaction points from the field case histories and brings the CSR values in line with V_{s1} value for sand as predicted by the Kayen et al. (2013) probability curves.
- 3. A simplified magnitude scaling factor (MSF) vs. moment magnitude M_w equation has been developed exclusively for gravel liquefaction. The MSF vs. M_w curve plots about mid-way between similar curves proposed for V_s methods for sands (Andrus and Stokoe, 2000 and Kayen et al. 2013) and is slightly below the lower bound MSF curve recommended for sand by the NEESR/NSF panel (Youd et al. 2001). These results suggest that the effect of magnitude on liquefaction resistance is similar for both sands and sandy gravels.
- 4. Although the probabilistic triggering curves for gravel are similar to those for sands (Kayen et al. 2013) at low V_{s1} values typical of loose gravels ($\approx 150 \text{ m/s}$), they shift to the right as V_{s1} values increase. This indicates that gravels can still liquefy at high V_{s1} values and the typical sand-based V_s triggering curves would incorrectly estimate these points as no liquefaction events.

DATA AVAILABILITY

Some or all data, models, or code that support the findings of this study are available from the corresponding author upon reasonable request. These data include electronic versions of gravel liquefaction database listed in Supplemental Table S1.

ACKNOWLEDGEMENTS

Funding for this study was provided by grant G16AP00108 from the US Geological Survey Earthquake Hazard Reduction Program and grants CMMI-1663546 and CMMI-1663288 from the National Science Foundation. This funding is gratefully acknowledged. This work is also part of a Research Project funded by ReLUIS (University Network of Seismic Engineering Laboratories) Consortium 2019-2021, WP 16 Geotechnical Engineering, Task 16.1 Site response and liquefaction. However, the opinions, conclusions and recommendations in this paper do not necessarily represent those of the sponsors. We also express sincere appreciation to Luca Minarelli for help in arranging access for geophysical surveys at sites in Italy and to G. Athanasopoulos for arranging access for these tests at sites in Cephalonia, Greece.

REFERENCES

- Amoroso, S., Barbača, J., Belić, N., Kordić, B., Brčić, V., Budić, M., Civico, R., De Martini, P.
 M., Hećej, N., Kurečić, T., Minarelli, L., Novosel, T., Palenik, D., Pantosti, D., Pucci, S.,
 Filjak, R., Ricci, T., Špelić, M., and Vukovski, M. (2021). Liquefaction field reconnaissance
 following the 29th December 2020 Mw 6.4 Petrinja earthquake (Croatia), EGU General Assembly 2021, online, 19–30 Apr 2021, EGU21-16584, https://doi.org/10.5194/egusphere-egu21-16584.
 - Andrus, R.D. (1994). "In situ characterization of gravelly soils that liquefied in the 1983 Borah

- Peak earthquake." Ph.D. Dissertation, Civil Engineering Dept., Univ. of Texas at Austin,
- 685 579 pp.
- Andrus, R.D., and Stokoe, K.H., II (2000). "Liquefaction resistance of soils from shear-wave ve-
- 687 locity." J. Geotech. Eng., 10.1061/(ASCE)1090-0241(2000)126:11(1015).
- Andrus, R.D. Hayati, H., and Mohanan, N.P. (2009). "Correcting liquefaction resistance for aged
- sands using measured to estimated velocity ratio." J. Geotech. Geoenviron. Eng., ASCE,
- Washington, D.C., 135(6): 735-744, DOI: 10.1061/_ASCE_GT.1943-5606.0000025.
- Arai, H., and K. Tokimatsu (2005). S-wave velocity profiling by joint inversion of microtremor
- dispersion curve and horizontal-to-vertical (H/V) spectrum, Bulletin of Seismological Soci-
- 693 ety of America, 95, 1766 1778, doi:10.1785/0120040243
- 694 Athanasopoulos-Zekkos, A., Zekkos, D., Rollins, K.M., Hubler, J., Higbee, J., Platis, A. (2019).
- 695 "Earthquake performance and characterization of gravel-size earth fills in the ports of Ceph-
- alonia, Greece, following the 2014 Earthquakes." Earthquake Geotechnical Engineering for
- Protection and Development of Environment and Constructions, Procs. 7th Intl. Conf. on
- Earthquake Geotechnical Engineering, Taylor and Francis, p. 1212-1219.
- Baratta, M., 1910. "La Catastrofe Sismica Calabro-Messinese (28 dicembre 1908)." Roma: Società
- Geografica Italiana.
- Bard, P. Y., Cadet, H., Endrun, B., Hobiger, M., Renalier, F., Theodulidis, N., ... & Kristeková,
- M. (2010). From non-invasive site characterization to site amplification: recent advances in
- the use of ambient vibration measurements. *Earthquake Engineering in Europe*, 105-123.
- Bindi, D., Pacor, F., Luzi, L., Puglia, R., Massa, M., Ameri, G., and Paolucci, R. (2011). "Ground
- motion prediction equations derived from the Italian strong motion database." Bulletin of
- 706 *Earthquake Engineering*, 9(6): 1899-1920.

- 707 Boulanger, R.W. and Idriss, I.M. (2014). "CPT and SPT based liquefaction triggering procedures."
- 708 Center of Geotechnical Modeling, Univ. of California-Davis, Report No. UCD/CGM-14/01.
- 709 Cao, Z., Youd, T.L., and Yuan, X. (2011). "Gravelly soils that liquefied during 2008 Wenchuan,
- 710 China Earthquake, Ms=8.0." *Soil Dynamics and Earthquake Engineering*, 31(8), 1132-1143.
- 711 Cao, Z., Youd, T., and Yuan, X. (2013). "Chinese Dynamic Penetration Test for liquefaction eval-
- 712 uation in gravelly soils." *J. Geotech. Eng.*, 10.1061/(ASCE)GT.1943-5606.0000857.
- 713 Cao, Z., Yuan, X., Youd, T.L., and Rollins, K.M. (2012). "Chinese Dynamic Penetration tests
- 714 (DPT) at liquefaction sites following 2008 Wenchuan Earthquake." Proc., 4th Int. Conf. on
- Geotechnical and Geophysical Site Characterization, Taylor & Francis Group, London,
- 716 1499-1504.
- 717 Chang, W.J. (2016). "Evaluation of liquefaction resistance for gravelly sands using gravel content-
- 718 corrected shear-wave velocity." *J. Geotech. Eng.*, 10.1061/(ASCE)GT.1943-5606.0001427.
- 719 Chen, L., Yuan, X., Cao, Z., Sun, R., Wang, W., & Liu, H. (2018). "Characteristics and triggering
- conditions for naturally deposited gravelly soils that liquefied following the 2008 Wenchuan
- Mw 7.9 earthquake, China". Earthquake Spectra, 34(3), 1091-1111.
- 722 Chu, B.L., Hsu, S.C., Lai, S.E., and Chang, M.J. (2000). "Soil Liquefaction Potential Assessment
- of the Wu feng Area after the 921 Chi-Chi Earthquake." Report of National Science Council
- 724 (in Chinese).
- 725 Coulter, H.W., and Migliaccio, R.R. (1966). "Effect of the Earthquake of March 22, 1964 at Val-
- dez. Alaska." U.S. Geological Survey Professional Paper 542-C.
- Cubrinovski, M., Bray, J., de la Torre, C., Olsen, 4. M., Bradley, B., Chiaro, G., ... & Wotherspoon,
- L. (2017). "Liquefaction effects and associated damages observed at the Wellington Cen-

- trePort from the 2016 Kaikōura earthquake." Bulletin of the New Zealand Society for Earthquake Engineering, 50 (2), 152-173.
- Cubrinovski, M., Bray, J.D., de la Torre, C., Olsen, M., Bradley, B., Chiaro, G., Stocks, E., Woth-
- erspoon, L., and Krall, T. (2018). "Liquefaction-Induced Damage and CPT Characterization
- of the Reclamations at CentrePort, Wellington Liquefaction-Induced Damage and CPT
- Characterization of the Reclamations at CentrePort, Wellington." Bulletin of the Seismolog-
- 735 ical Society of America, 108(3B): 1695-1708.
- DeJong, J.T., Ghafghazi, M., Sturm, A.P., Wilson, D.W., den Dulk, J., Armstrong, R.J., Perez, A.,
- and Davis, C.A. (2017). "Instrumented Becker Penetration Test. I: Equipment, Operation,
- 738 and Performance." J. Geotech. Eng., doi.org/10.1061/(ASCE)GT.1943-5606.0001718.
- Dobry, R., Ladd, R., Yokel, F., Chung, R. & Powell, D. (1982). Prediction of pore water pressure
- buildup and liquefaction of sands during earthquakes by the cyclic strain method. NBS
- Huilding Science Series 138, National Bureau of Standards, Washington, DC.
- Faenza, L., & Michelini, A. (2011). "Regression analysis of MCS intensity and ground motion
- spectral accelerations (SAs) in Italy." Geophysical Journal International, 186(3), 1415-
- 744 1430.
- Fäh, D., Kind, F., & Giardini, D. (2003). Inversion of local S-wave velocity structures from aver-
- age H/V ratios, and their use for the estimation of site-effects. Journal of Seismology, 7(4),
- 747 449-467.
- 748 Foti S, Comina C, Boiero D, Socco LV (2009). "Non-uniqueness in surface wave inversion and
- consequences on seismic site response analyses." Soil Dynamics and Earthquake Engineer-
- 750 ing 29(6):982–993

- 751 Franke, K.W. and Rollins, K.M. (2017). "Lateral spread displacement and bridge foundation case
- histories from the 1991 M7.6 Earthquake near Limón, Costa Rica." J. Geotechnical and Ge-
- oenvironmental Engineering, ASCE, Vol. 143, No. 6, 17 p.
- Garofalo, F. Foti, S., Hollender, F., Bard, P.Y., Cornou, C., Cox, B. R., Ohrnberger, M., Sicilia,
- D., Asten, M., Di Giulio, G., Forbriger, T., Guillier, B., Hayashi, K., Martin, A.,
- 756 Matsushima, S., Mercerat, D., Poggi, V., Yamanaka, H. (2016). "InterPACIFIC project:
- Comparison of invasive and non-invasive methods for seismic site characterization. Part I:
- Intra-comparison of surface wave methods." Soil Dyn. and Earthquake Eng., 82(3), 222-
- 759 240.
- Garofalo, F. Foti, S., Hollender, F., Bard, P.Y., Cornou, C., Cox, B. R., Ohrnberger, M., Sicilia,
- D., Asten, M., Di Giulio, G., Forbriger, T., Guillier, B., Hayashi, K., Martin, A.,
- Matsushima, S., Mercerat, D., Poggi, V., Yamanaka, H. (2016). "InterPACIFIC project: In-
- tercomparison of invasive and non-invasive methods for seismic site characterization. Part
- II: Intra-comparison between surface-wave and borehole methods." Soil Dyn. and Earth-
- 765 quake Eng., 82(3), 241-254.
- Golesorkhi, R. (1989). "Factors influencing the computational determination of earthquake-in-
- duced shear stresses in sandy soils." PhD dissertation, University of California, Berkeley,
- 768 California.
- Harder, L.F. (1997). "Application of the Becker Penetration Test for evaluating the liquefaction
- potential of gravelly soils." NCEER Workshop on Evaluation of Liquefaction Resistance,
- held in Salt Lake City, Utah.

- Harder, L.F., Jr., and Seed, H.B. (1986). "Determination of penetration resistance for coarse-
- grained soils using the Becker Hammer Drill." College of Engineering, University of Cali-
- fornia, Berkeley, Calif. Rep. No. UCB/EERC-86/06. May 1986.
- Hubler, J., Athanasopoulos-Zekkos, A., and Zekkos, D. (2018). "Monotonic and cyclic simple
- shear response of gravel-sand Mixtures", Soil Dynamics and Earthquake Engineering, Vol
- 777 115, pp. 291-304, Dec 2018, https://doi.org/10.1016/j.soildyn.2018.07.016
- Hubler, J., Athanasopoulos-Zekkos, A., and Zekkos, D. (2017). "Monotonic, cyclic and post-cy-
- clic simple shear response of three uniform gravels in constant volume conditions", J. Ge-
- otech. and Geoenviron Eng. ASCE, Washington, DC, 143(9) doi 10.1061/(ASCE)GT.1943-
- 781 5606.0001723
- 782 Idriss, I.M. (1999). "An update to the Seed-Idriss simplified procedure for evaluating liquefaction
- potential." Procs. TRB Workshop on New Approaches to Liquefaction, Publication No.
- 784 FHWA-RD-99-165, Federal Highway Administration.
- 785 Idriss, I. and Boulanger, R. W. (2008). "Soil liquefaction during earthquakes." Earthquake Engi-
- 786 neering Research Institute.
- 787 Ishihara, K. (1985). "Stability of natural deposits during earthquakes." *Proc.*, 11th Int. Conf. on
- 788 *Soil Mech. and Found. Eng.*, 1, 321-376.
- Jamiolkowski, M. and Lo Presti, D. C. F. (1990). "Correlation between liquefaction resistance and
- shear wave velocity." Soils and Foundations, Japanese Soc. Soil Mechanics, Tokyo, 32(2),
- 791 145-148.
- Juang, C. H., Chen, C. J., and Jiang, T. (2001). "Probabilistic framework for liquefaction potential
- by shear wave velocity." J. Geotech. Geoenviron. Eng., 127(8), 670–678.

- Juang, C. H., Jiang, T., and Andrus, R. D. (2002). "Assessing probability based methods for lique-
- faction evaluation." J. Geotech. Geoenviron. Eng., 128(7), 580–589.
- Kayen, R., Moss, R.E.S., Thompson, E.M., Seed, R.B., Cetin, K.O., Der Kiureghian, A., Tanaka,
- Y., and Tokimatsu, K. (2013). "Shear-wave velocity-based probabilistic and deterministic
- 798 assessment of seismic soil liquefaction potential." J. Geotech. Eng.,
- 799 doi.org/10.1061/(ASCE)GT.1943-5606.0000743.
- Kayen, R. E., Mitchell, J. K., Seed, R. B, Lodge, A., Nishio, S., and Coutinho, R. (1992). "Evalu-
- ation of SPT-, CPT-, and shear wave-based methods for liquefaction potential assessment
- using Lom Prieta data." In Proc., 4th Japan-U.S. Workshop on Earthquake Resistant Des. of
- Lifeline Fac. and Countermeasures for Soil Liquefaction, Tech. Report NCEER-92-0019
- Vol. 1 National Center for Earthquake Engineering Research, Buffalo, 177-204.
- Kayen, R., Tanaka, E. Y., Kishida T., and Sugimoto, S. (2002). "Liquefaction potential of native
- ground in West Kobe, Japan by the spectral analysis of surface waves (SASW) method."
- Proc., 8th U.S.-Japan Workshop on Earthquake Resistant Design of Lifeline Facilities and
- 808 Countermeasures against Liquefaction. Tokyo.
- Kokusho, T., Tanaka, Y., Kudo, K., and Kawai, T. (1995). "Liquefaction case study of volcanic
- gravel layer during 1993 Hokkaido-Nansei-Oki earthquake." Proc., 3rd Int. Conf. on Recent
- 811 Advances in Geotech. Earthquake Eng. and Soil Dyn., 235-242.
- Kokusho, T., and Yoshida, Y. (1997). "SPT N-value and S-wave velocity for gravelly soils with
- different grain size distribution." Soils and Foundations, 37(4): 105-113.
- 814 Kozeny, J. (1927). Ueber kapillare Leitung des Wassers im Boden. Sitzungsber Akad. Wiss.,
- 815 Wien, 136(2a): 271-306.
- 816 Kramer, S. L. (1996). Geotechnical Earthquake Engineering, Prentice-Hall, 653 p.

- Liao, S. S. C, Veneziano, D., Whitman R.V. (1988). "Regression models for evaluating liquefac-
- tion probability." J. Geotech. and Geoenviron. Eng., ASCE, 114(4), 389-411.
- Liao, S., and Whitman, R. V. (1986). "Overburden correction factors for SPT in sand." J. Ge-
- 820 *otech. Engrg.*, ASCE, 112(3), 373–377.
- Lodge, A. L. (1994). "Shear wave velocity measurements for subsurface characterization." Ph.D.
- Dissertation, Univ. of California, Berkeley, California. Lopez, S., Vera-Grunauer, X.,
- Rollins, K., and Salvatierra, G. (2018). "Gravelly soil liquefaction after the 2016 Ecuador
- Earthquake." Proc., Conf. on Geotechnical Earthquake Engineering and Soil Dynamics V,
- 825 273-285.
- 826 Lopez, S., Vera-Grunauer, X., Rollins, K., and Salvatierra, G. (2018). "Gravelly soil liquefaction
- after the 2016 Ecuador Earthquake." *Proc., Conf. on Geotechnical Earthquake Engineering*
- 828 *and Soil Dynamics V*, 273-285.
- Maurenbrecher P.M., Den Outer, A., and Luger, H.J. (1995). "Review of geotechnical investiga-
- tions resulting from the Roermond April 13, 1992 earthquake.", Proc. 3rd Int. Conf. on Re-
- 831 cent Advances in Geotech. Earthquake Eng. and Soil Dyn., 645-652.
- McCulloch, D. S., & Bonilla, M. G. (1970). "Effects of the earthquake of March 27, 1964, on the
- Alaska Railroad". US Government Printing Office.
- Morales, C, Ledezma, C., Saez, E., Boldrini, S., and Rollins, K.M., 2020. "Seismic failure of an
- old pier during the 2014 Mw8.2, Pisagua, Chile earthquake." Earthquake Spectra, EERI,
- https://journals.sagepub.com/doi/10.1177/8755293019891726
- Nikolaou, S., Zekkos, D., Assimaki, D., and Gilsanz, R. (2014). "GEER/EERI/ATC Earthquake
- Reconnaissance January 26th/February 2nd 2014 Cephalonia, Greece Events, Version

839	1."http://www.geerassociation.org/index.php/component/geer_reports/?view=geerre-
840	ports&id=32
841	Ohta, Y. and Goto, N. (1978). "Physical background of the statistically obtained S-wave velocity
842	equation in terms of soil indexes." ButsuriTanko(Geophysical Exploration), Tokyo, Japan,
843	31(1), 8-17 (In Japanese).
844	Park, C.B., Miller, R.D, and Xia J. (1999). "Multichannel analysis of surface waves." Geophysics,
845	64: 800–808.
846	Pavlides, S., Muceku, Y., Chatzipetrow, A., Georgious, G., Lazos, I. 2020. "Preliminary report on
847	the ground failures of the Albanian (Durres-Thumane) 26th of November Earthquake.
848	Picozzi, M., S. Parolai, and S. M. Richwalski (2005). "Joint inversion of H/V ratios and disper-
849	sion curves from seismic noise: Estimating the S-wave velocity of bedrock." Geophysical
850	Research Letters, 32, L11308, doi:10.1029/2005GL022878.
851	Robertson, P.K. and Woeller, D.J. and Finn, W.D.L. (1992). "Seismic cone penetration test for
852	evaluating liquefaction potential", Canadian Geotechnical Journal, 29(4) 686-695.
853	Rollins, K.M., Amoroso, S., Milan, G., Minerelli, L., Vassallo, M., Di Giulio, G. (2020). "Gravel
854	liquefaction assessment using the dynamic cone penetration test based on field perfor-
855	mance from the 1976 Friuli earthquake." J. Geotech. and Geoenviron. Eng., ASCE,
856	https://DOI.org/10.1061/(ASCE)GT.1943-5606.0002252.
857	Rollins, K.M., Diehl, N.B. and Weaver, T.J. (1998a) "Implications of V _s -BPT (N ₁) ₆₀ Correlations
858	for Liquefaction Assessment in Gravels." Proc. Geotechnical Earthquake Engineering and
859	Soil Dynamics, Geotech. Special Pub. No. 75, ASCE, 1, 506-517.
860	Rollins, K.M., Evans, M., Diehl, N. and Daily, W. (1998b). "Shear modulus and damping rela-
861	tionships for gravels." J. Geotech. and Geoeviron. Eng, ASCE, 124(5) p. 396-405.

- Rollins, K.M., Ledezma, C., and Montalva, G., Becerra, A., Candia, G., Jara, D., Franke, K., Saez,
- E. (2014). Geotechnical Aspects of April 1, 2014, M8.2 Iquique, Chile Earthquake." *GEER*
- Association Report No. GEER-038, 77 p. Version 1.2: October 22, 2014
- Seed, H. B., and Idriss, I. M. (1971). "Simplified procedure for evaluating soil liquefaction poten-
- 866 tial." J. Geotech. Engrg. Div., ASCE, 97(9),1249–1273.
- Seed, H. B., Martin, P. P. & Lysmer, J. (1976). "The generation and dissipation of pore water
- pressure changes during soil liquefaction". J. Geotech. Eng. Div., 102(4), 323-346.
- 869 Seed, H. B., Idriss, I. M., and Arango, I. (1983). "Evaluation of liquefaction potential using field
- performance data." *J. Geotech. Eng.*, 109(3), 458–482.
- 871 She, K., Horn, D. P. D. P., and Canning, P. (2006). "Porosity and hydraulic conductivity of mixed
- sand-gravel sediment". Flood and Coastal Risk Management, At York, 1-16.
- 873 Sirovich, L. (1996a). "Repetitive Liquefaction at gravelly site and liquefaction in overconsolidated
- 874 sands." *Soils and Foundations*, (36)4, 23-34.
- Sirovich, L. (1996b). "In-situ testing of repeatedly liquefied gravels and liquefied overconsolidated
- 876 sands." *Soils and Foundations*, (36)4, 35-44.
- 877 Stokoe, K. H. II, Wright, S. G., Bay, J. A., and Roesset, J. M. (1994). "Characterization of ge-
- otechnical sites by SASW method," ISSMFE, Technical Committee #10 for XIII ICSMFE,
- Geophysical Characterization of Sites, A. A. Balkema Publishers/Rotterdam & Brookfield,
- Netherlands, 15–25.
- 881 Sykora, D. W. 1987. "Creation of a data base of seismic shear wave velocities for correlation
- analysis." Geotech. Lab. Misc. Paper GL-87-26, U.S. Army Engr. Waterways Experiment
- Station, Vicksburg, Miss.

- Tokimatsu, K. 1997. "Geotechnical site characterization using surface waves." Earthquake Ge-
- otechnical Engineering, A.A. Balkema, Brookfield, Vt., 1333-1368.
- Tokimatsu, K., and Yoshimi, Y. 1983. "Empirical correlation of soil liquefaction based on SPT N-
- value and fines content." Soils and Foundations, 23(4), 56-74.
- Vantassel J, Cox B, Wotherspoon L and Stolte A 2018. "Deep shear wave velocity profiling and
- fundamental site period measurements at CentrePort, Wellington and implications for locate
- site amplification". Bulletin of the Seismological Society of America, 108 (3).
- Vantassel, J. P., and Cox, B. R. (2021). "A procedure for developing uncertainty-consistent V_s
- profiles from inversion of surface wave dispersion data." Soil Dynamics and Earthquake
- 893 Engineering, 145, 106622.
- Wang, W.S. 1984. "Earthquake damages to earth dams and levees in relation to soil liquefaction
- and weakness in soft clays." In Proc. Intl. Conf. on Case Histories in Geotech. Eng., 1, 511-
- 896 521.
- Wathelet, M., D. Jongmans, and M. Ohrnberger (2004). Surface-wave inversion using a direct
- search algorithm and its application to ambient vibration measurements. Near surface geo-
- 899 physics 2.4: 211-221.
- 900 Weston, T. R. 1996. "Effects of grain size and particle distribution on the stiffness and damping
- of granular soils at small strains." MS thesis, University of Texas, Austin, Texas.
- Worden, C. B., Wald, D. J., Allen, T. I., Lin, K., and Cua, G. 2010. "Integration of macroseismic
- and strong-motion earthquake data in ShakeMap for real-time and historic earthquake anal-
- ysis." USGS website, http://earthquake.usgs.gov/earthquakes/shakemap/.
- Yegian, M.K., Ghahraman, V.G., and Harutiunyan, R.N., 1994. "Liquefaction and embankment
- failure case histories, 1988 Armenia earthquake." J. Geotech. Eng., 10.1061/(ASCE)0733-

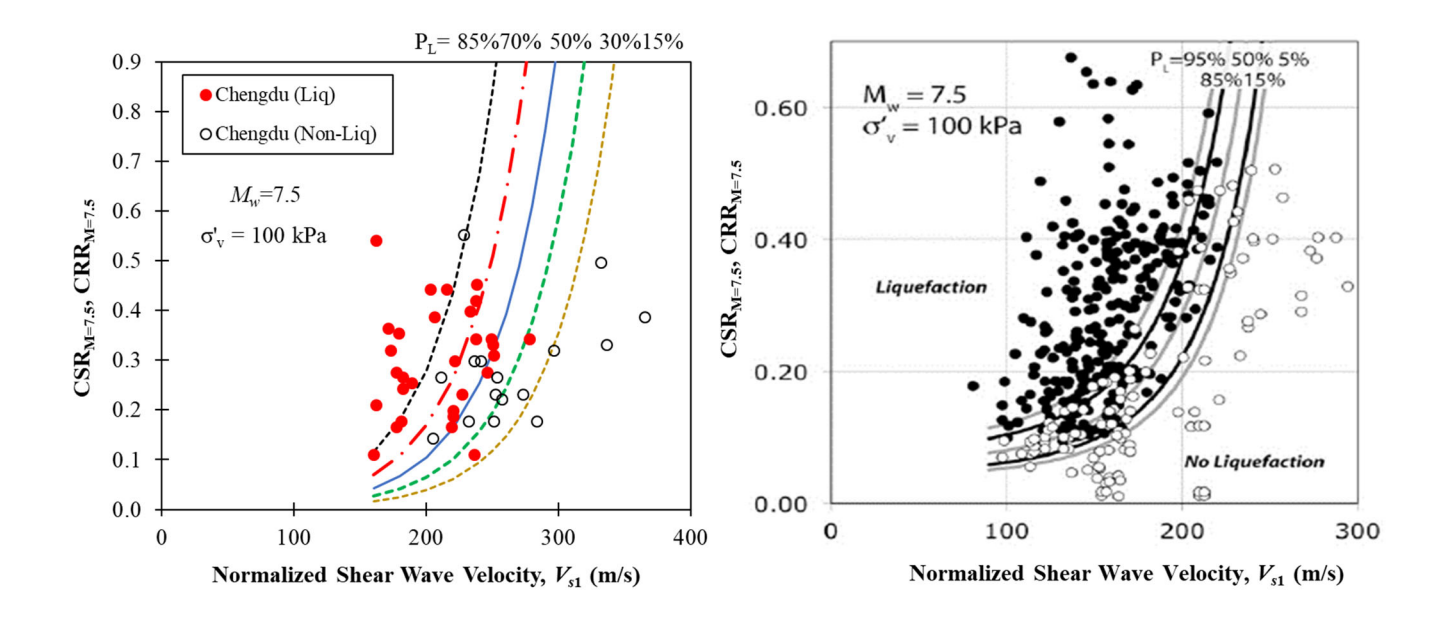
- 907 9410(1994)120:3(581).
- 908 Youd, T.L. and Hoose, S.N. 1978. "Historic ground failures in Northern California triggered by
- earthquakes." U.S. Geological Survey Professional Paper 1993, 180 p.
- 910 Youd, T.L., Harp, E.L., Keefer, D.K., and Wilson, R.C. 1985. "The Borah Peak, Idaho Earthquake
- of October 29, 1983-Liquefaction." Earthquake Spectra, 2, 71-90.
- Youd, T. L., and Noble, S. K. 1997. "Magnitude scaling factors." In Proc., NCEER Workshop on
- 913 Evaluation of Liquefaction Resistance of Soils, Nat. Ctr. for Earthquake Engrg. Res., State
- 914 Univ. of New York at Buffalo, 149–165.
- 915 Youd, T.L., Idriss, I.M., Andrus, R.D., Arango, I., Castro, G., Christian, J.T., Dory, R., Finn,
- W.D.L., Harder, L.F., Hynes, M.E., Ishihara, K., Koester, J.P., Liao, S.S.C., Marcuson,
- 917 W.F., Martin, G.R., Mitchell, J.K., Moriwaki, Y., Power, M.S., Robertson, P.K., Seed, R.B.,
- and Stokoe, K.H. 2001. "Liquefaction resistance of soils: Summary Report from the 1996
- NCEER and 1998 NCEER/NSF Workshops on evaluation of liquefaction resistance of
- 920 soils." J. Geotech. Eng., 10.1061/(ASCE)1090-0241(2001)127:10(817).
- 21 Zhou, Y. G., Xia, P., Ling, D. S., and Chen, Y. M. (2020). Liquefaction case studies of gravelly
- soils during the 2008 Wenchuan earthquake. *Engineering Geology*, 274, 105691.

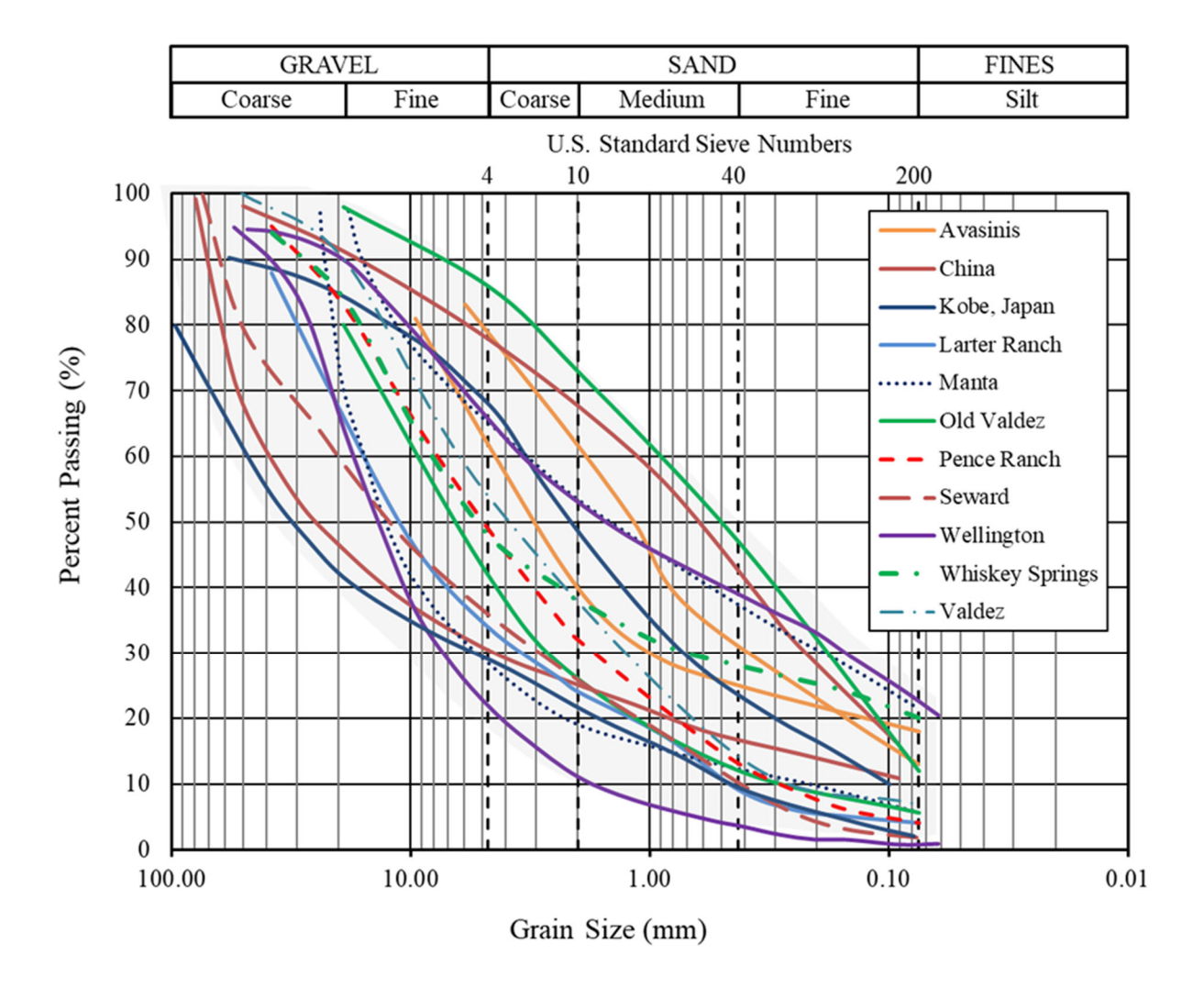
 Table 1. Case histories involving liquefaction of gravelly soil.

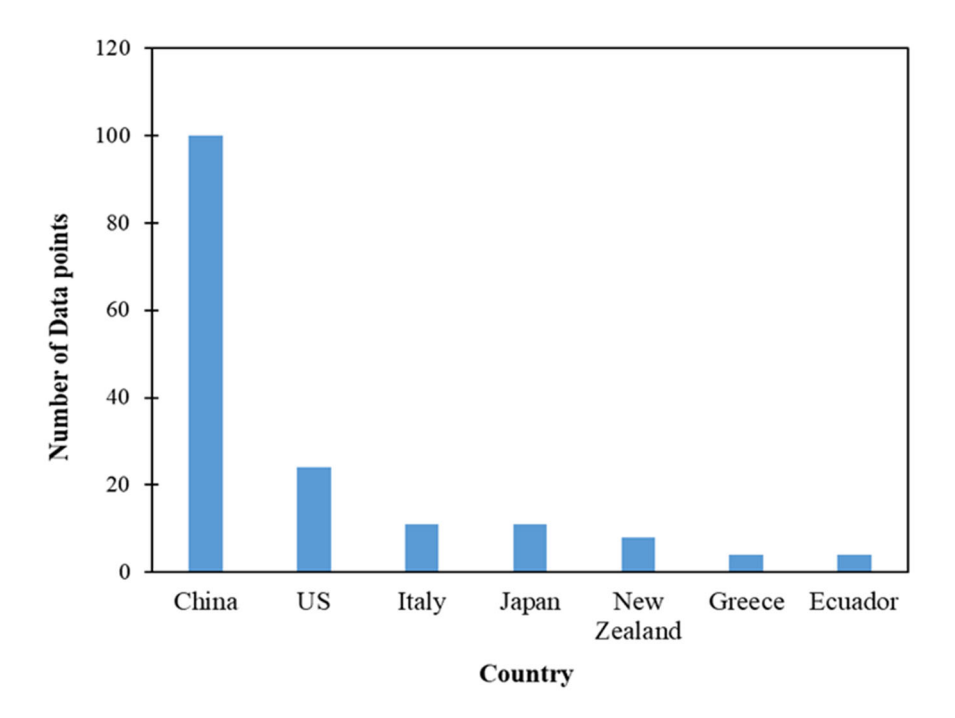
Earthquake	Year	$M_{\rm w}$	Reference	
Mino-Owari, Japan	1891	7.9	Tokimatsu and Yoshimi (1983)	
San Francisco, California	1906	8.2	Youd and Hoose (1978)	
Messina, Italy	1908	7.1	Baratta (1910)	
Fukui, Japan	1948	7.3	Ishihara (1985)	
Alaska, USA	1964	9.2	Coulter and Migliaccio (1966), McCulloch and Bonilla (1970)	
Haicheng, China	1975	7.3	Wang (1984)	
Tangshan, China	1976	7.8	Wang (1984)	
Friuli, Italy	1976	6.4	Sirovich (1996a, b), Rollins et al. (2020)	
Miyagiken-Oki, Japan	1978	7.4	Tokimatsu and Yoshimi (1983)	
Montenegro	1979	6.9	Kocui (2004)	
Borah Peak, Idaho, USA	1985	6.9	Youd et al. (1985), Andrus (1994), Harder and Seed (1986)	
Armenia	1988	6.8	Yegian et al. (1994)	
Limon, Costa Rica	1991	7.7	7 Franke and Rollins (2017)	
Roermond, Netherlands	1992	5.8	Maurenbrecher et al. (1995)	
Hokkaido, Japan	1993	7.8	Kokusho et al. (1995)	
Kobe, Japan	1995	7.2	2 Kokusho and Yoshida (1997)	
Chi-Chi, Taiwan	1999	7.8	Chu et al. (2000), Lin et al. (2004)	
Kocaeli, Turley	1999	7.6	Bardet et al. (2000)	
Wenchuan, China	2008	7.9	Cao et al (2011, 2013)	
Tohoku, Japan	2010	9.0	Tatsuoka et al. (2017)	
Cephalonia Is., Greece	2012	6.1	Nikolaou et al. (2014), Athanasopoulos-Zekkos et al. (2019, 2021)	
Iquique, Chile	2014	8.2	Rollins et al. (2014), Morales et al. (2020)	
Muisne, Ecuador	2016	7.8	Lopez et al. (2018)	
Kaikoura, New Zealand	2016	7.8	Cubrinovsky et al. (2017)	
Durres, Albania	2019	6.4	Pavlides et al. (2020)	
Petrinja, Croatia	2020	6.4	Amoroso et al. (2021)	

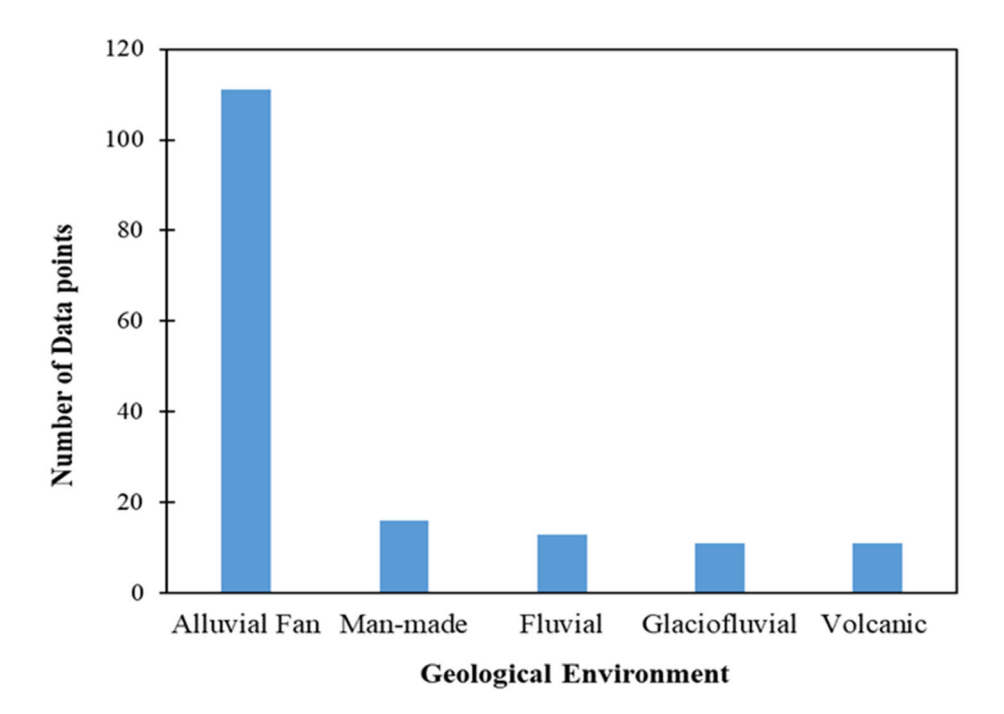
 Table 2: Results of model parameter estimates from logistic regression analysis.

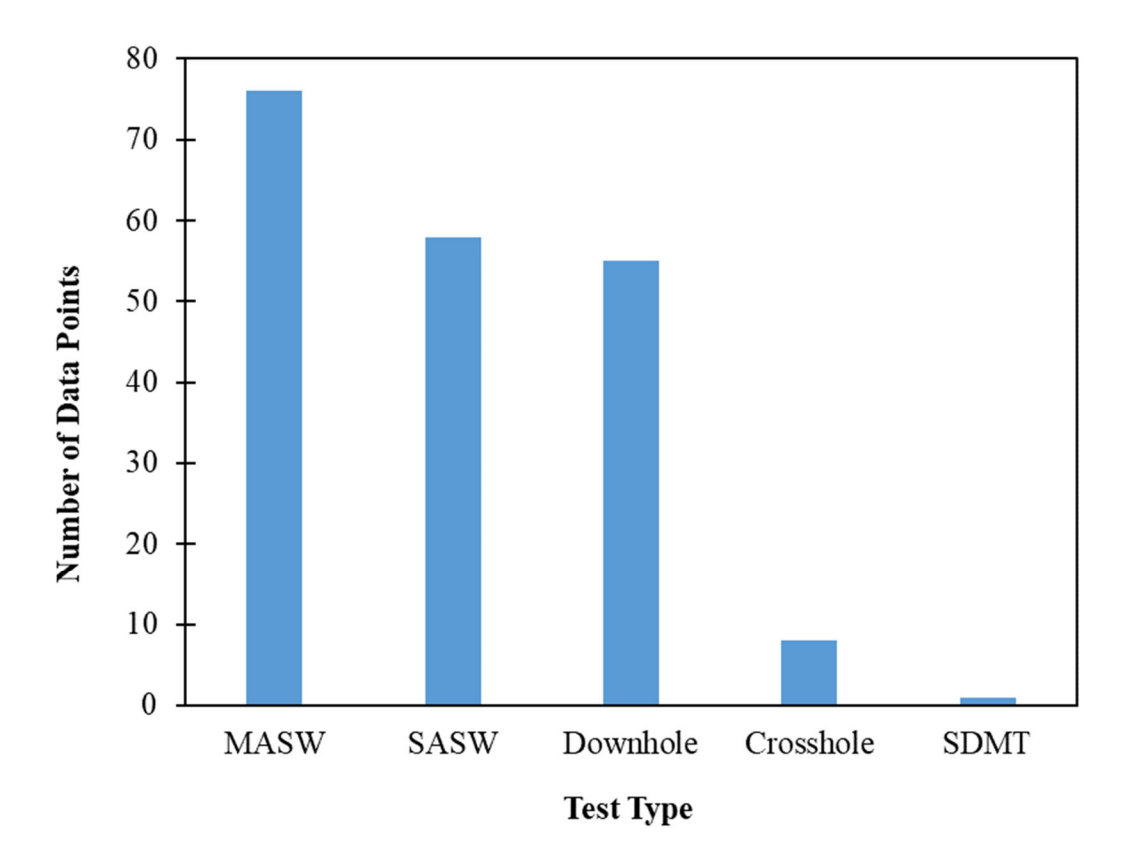
Candid	Parameter Estimates (p<0.05)					
variables	Trial 1	Trial 2	Trial 3	Trial 4		
V_{s1}	-0.048					
$V_{s,1}^{2}$	-	-1.48E-4				
$V_{s,1}^{3}$	-		-3.88E-7			
$V_{s,1}^{4}$				-1.3E-9		
$M_{\scriptscriptstyle W}$	2.02	2.01	1.6	1.52		
Ln(CSR)	3.046	5.11	4.95	5.152		

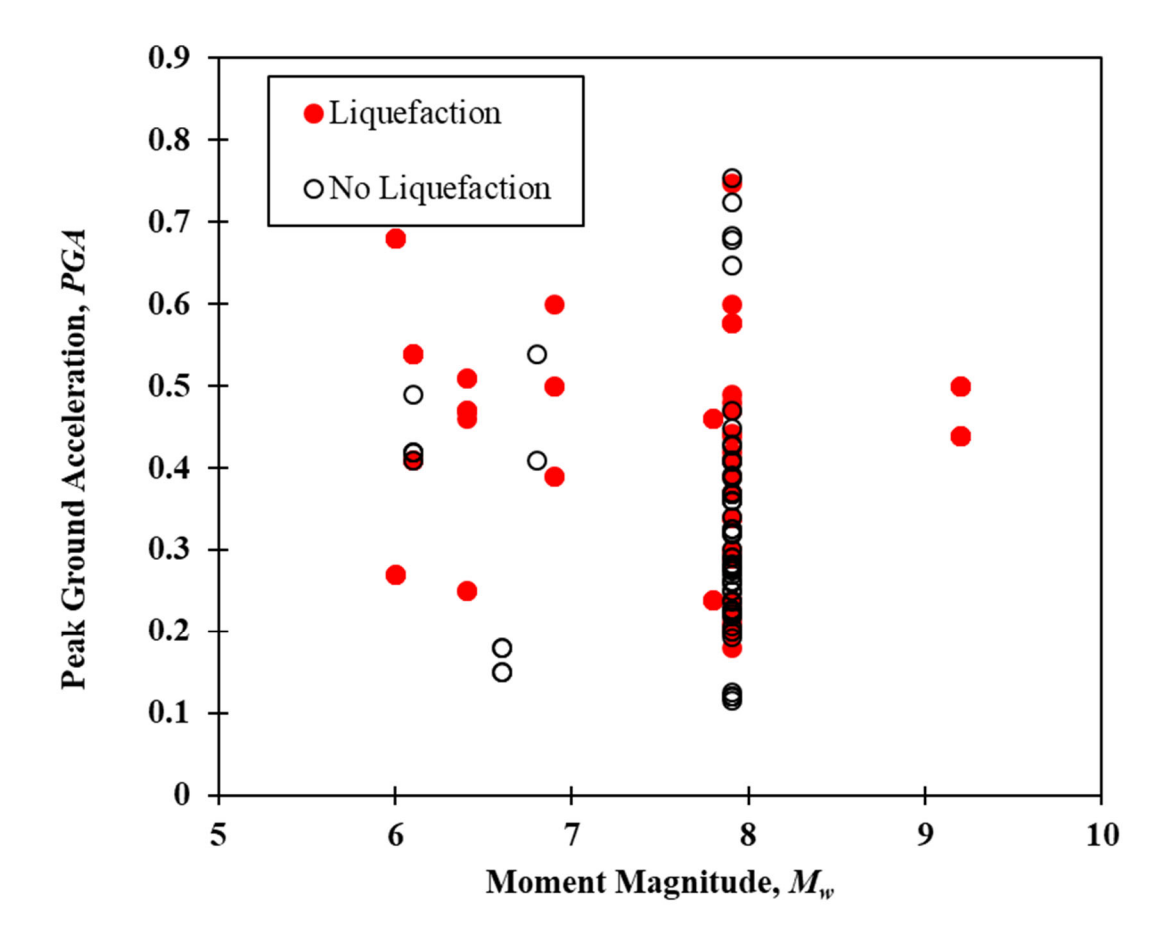




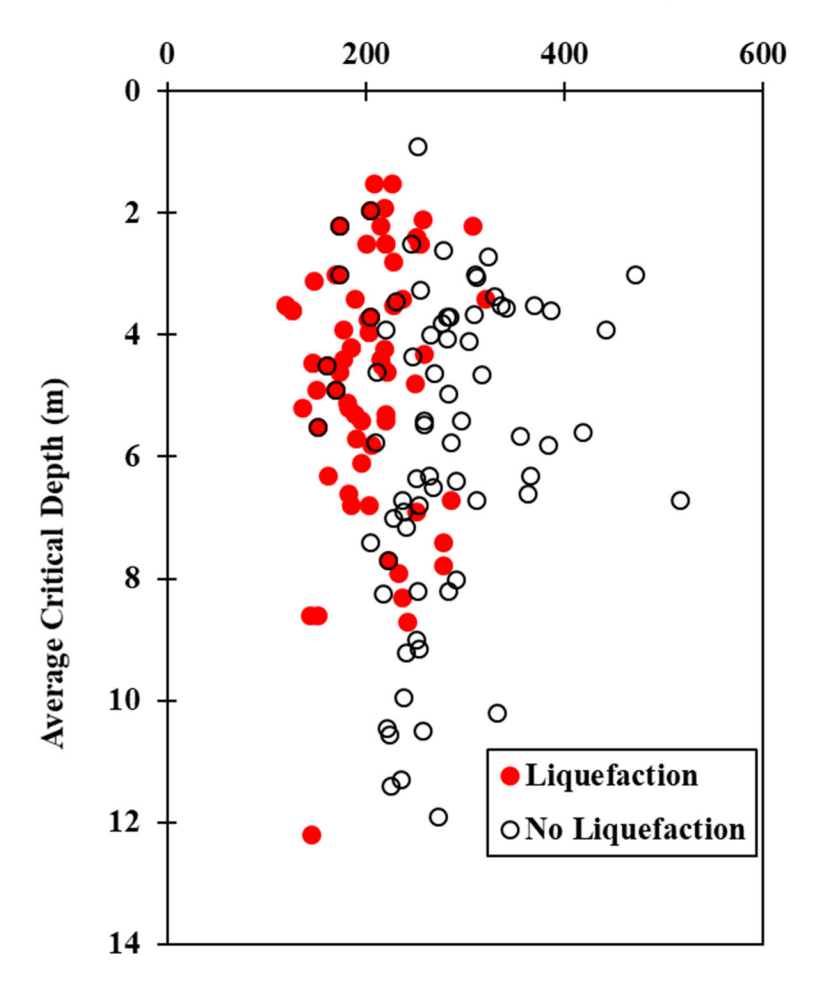


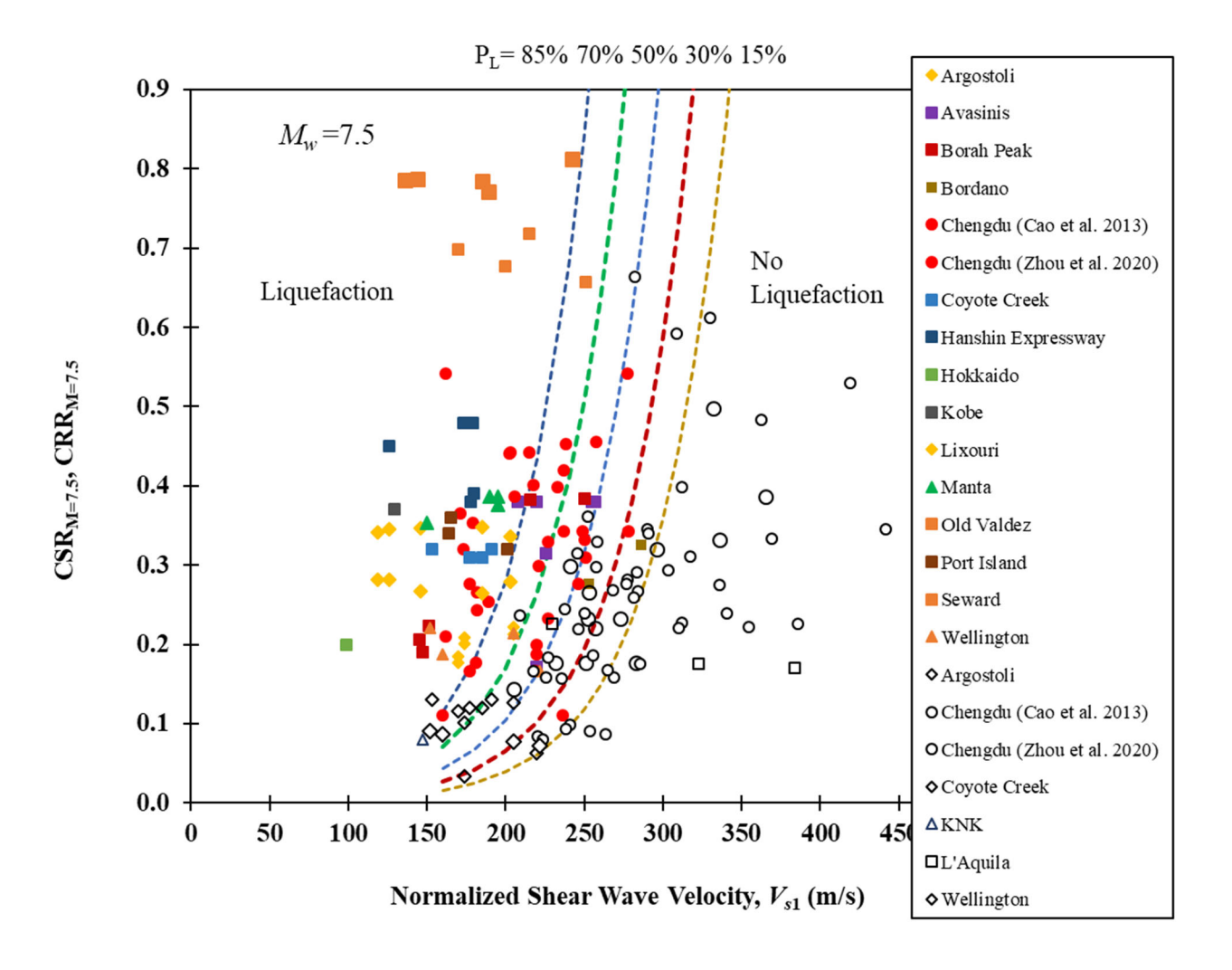


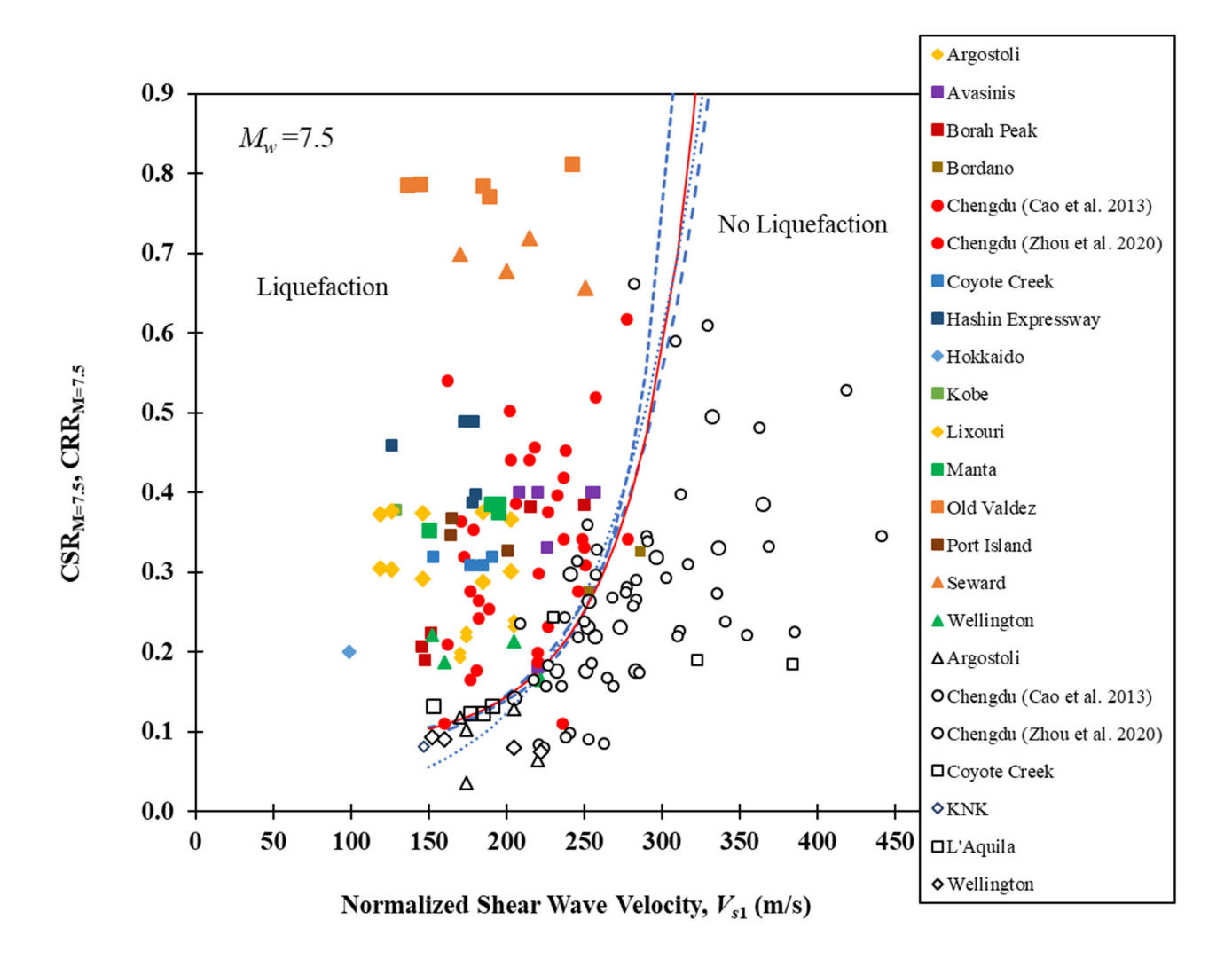


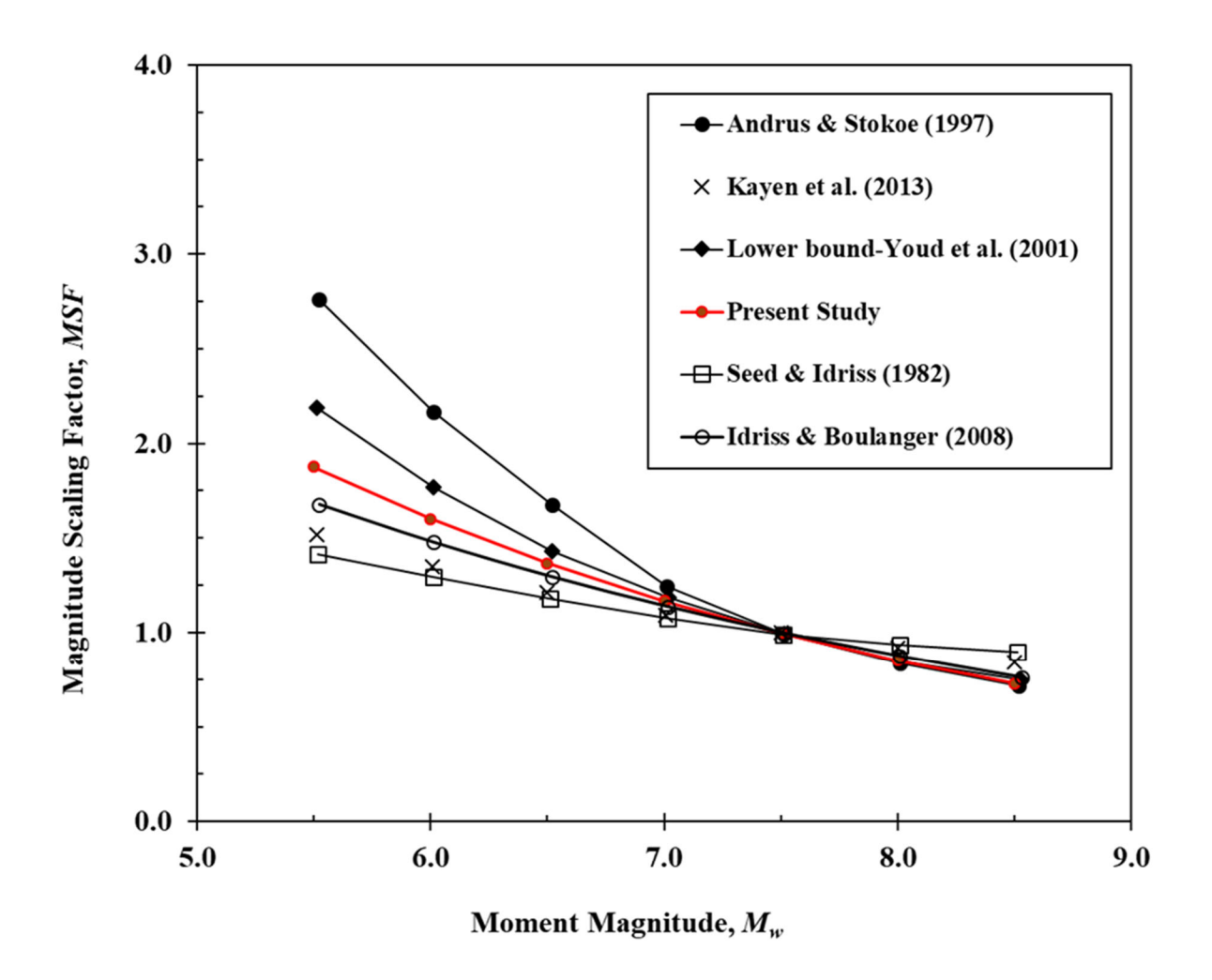


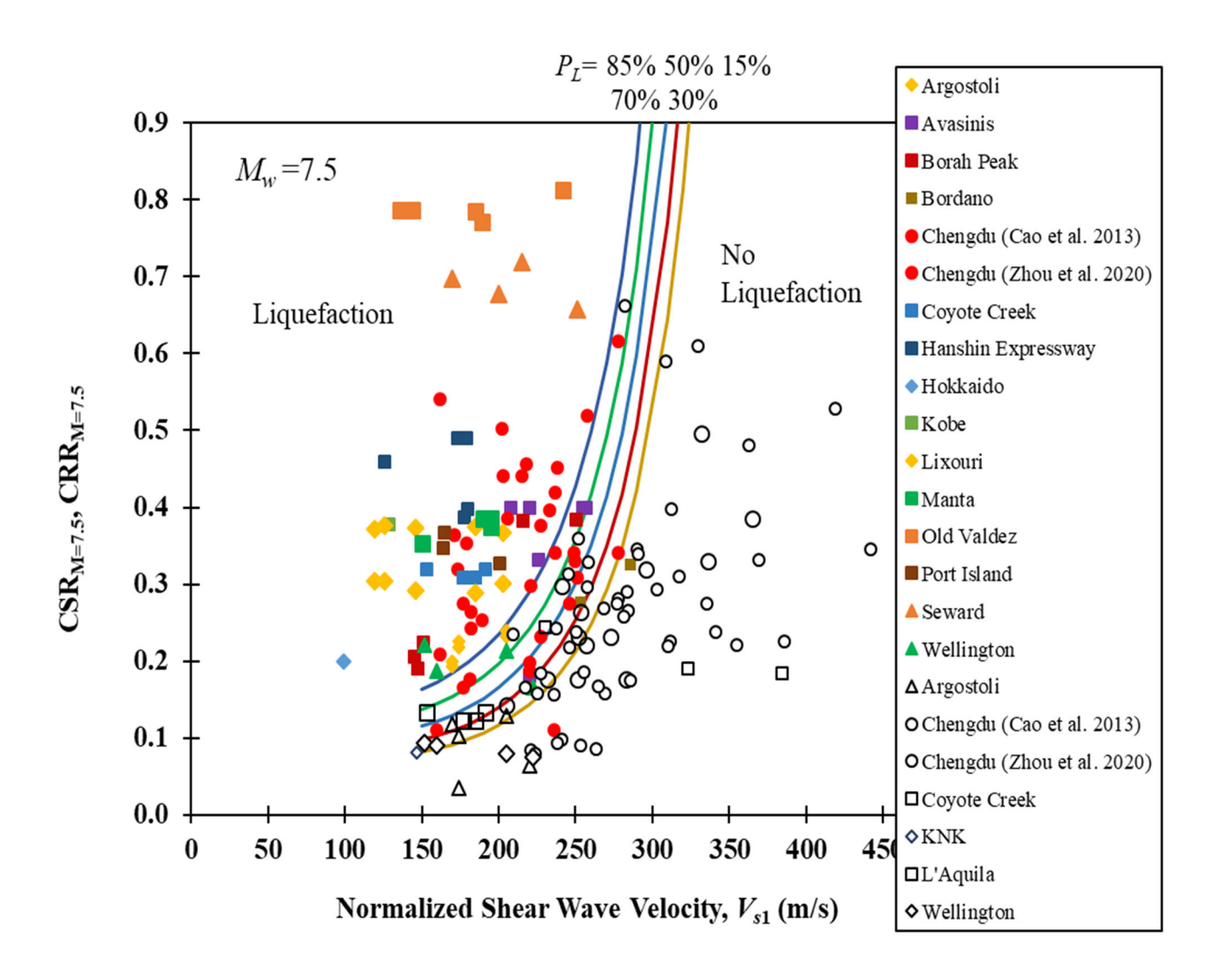
Normalized Shear Wave Velocity, V_{s1} (m/s)

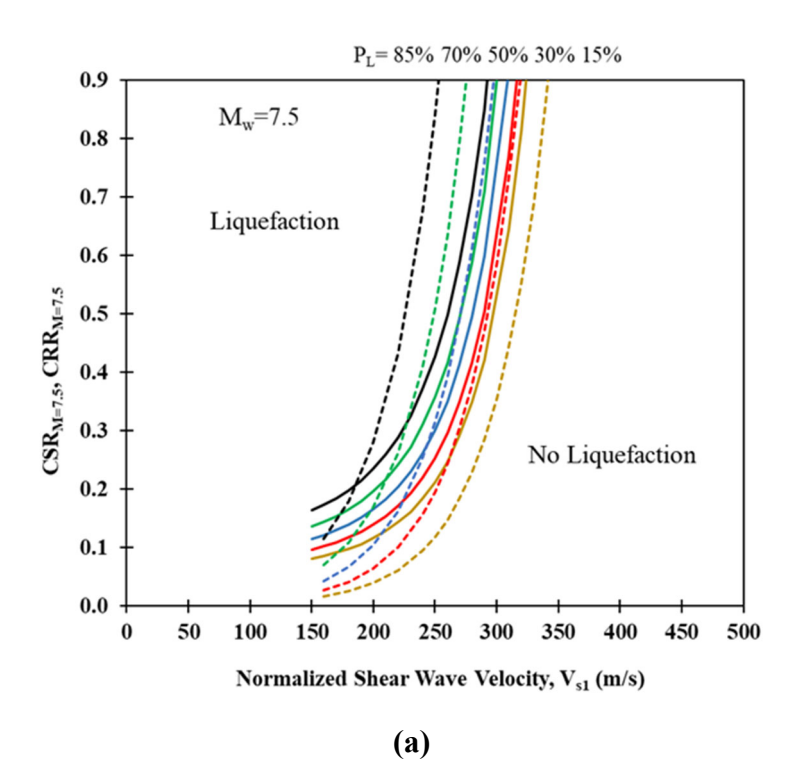


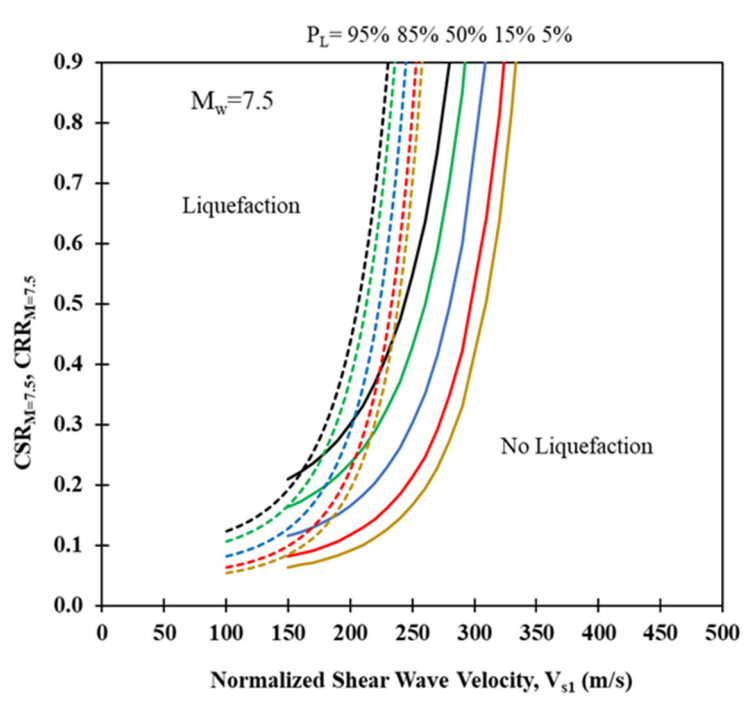












(b)